Far field operator splitting by principal component pursuit

Roland Griesmaier* and Lisa Schätzle†

December 15, 2025

Abstract

We consider scattering of time-harmonic plane waves by an ensemble of well-separated compactly supported inhomogeneous scatterers. The far field operator, which maps superpositions of plane wave incident fields to the far field patterns of the associated scattered fields, is commonly used as an idealized description of data sets obtained in corresponding remote sensing experiments. Suppose that some *a priori* information about the approximate position of just one of the scatterers in the ensemble is available. This article is about recovering the far field operator associated to this single scatterer from the far field operator associated to the whole collection of scatterers. Due to multiple scattering effects this is a nonlinear inverse problem. We show that an approximate solution can be obtained by decomposing the far field operator into a sparse component and a low-rank component, and we apply a convex program called principal component pursuit for this purpose. We give necessary and sufficient conditions for unique solvability, establish a stability result and provide numerical examples to illustrate our theoretical findings.

Mathematics subject classifications (MSC2010): 35R30 (65N21)
Keywords: Inverse medium scattering, Helmholtz equation, far field operator splitting, principal component pursuit
Short title: Far field operator splitting

1 Introduction

This article is concerned with far field operators for the scattering of scalar time-harmonic plane waves by compactly supported inhomogeneous obstacles. These operators are defined in terms of the far field patterns of scattered fields corresponding to plane wave incident fields at a single frequency for all possible observation and incident directions. Far field operators map densities of superpositions of such plane waves to the far field patterns of the associated scattered fields. They are a popular model for remote sensing observations in inverse scattering theory and their properties have been widely studied in the literature. It is, for instance, well known that the refractive index of a bounded penetrable scattering object is uniquely determined by the associated far field operator (see [4, 36, 38, 40]). Accordingly, far field operators are at the foundation of many successful reconstruction methods for the inverse medium scattering problem (see, e.g., [1, 10, 11, 14, 21, 30] and the monographs [5, 6, 13, 33]).

We shall study a particular data splitting problem for far field operators corresponding to ensembles of finitely many well-separated penetrable scatterers. Well-separated means here that

---

*Institut für Angewandte und Numerische Mathematik, Karlsruher Institut für Technologie, Englerstr. 2, 76131 Karlsruhe, Germany (`roland.griesmaier@kit.edu`).

†Department of Mathematics and System Analysis, Aalto University, P.O. Box 11100, 00076 Helsinki, Finland (`lisa.schatzle@aalto.fi`).

the diameters of the supports of the scatterers in the ensemble are small compared to their distances to each other. Assuming that the approximate locations of all scatterers in such an ensemble are available *a priori*, it has recently been shown in [22] that approximations of the far field operators associated to each scatterer individually can be recovered given the far field operator associated to the whole collection of scatterers. Due to multiple scattering between the different scatterers in the ensemble, which has to be disentangled and removed by the splitting method, this is a nonlinear inverse problem. The algorithms developed in [22] crucially rely on sparse representations of the far field operators corresponding to the individual scatterers in the ensemble, which are determined by the *a priori* information on their approximate locations. Using these sparse representations, either least squares or a convex program called basis pursuit (see, e.g., [9, 17, 18]) has been applied to recover the unknown far field operator components in [22].

In this work we aim to significantly reduce the required *a priori* information compared to [22]. We ask whether it is possible to extract the far field operator associated to a single scatterer in an ensemble of well-separated compactly supported scatterers from the far field operator associated to the whole ensemble, assuming that just the approximate location of this single scatterer is known, but nothing about the other scatterers. In other words, our goal is to isolate or split off the information about a single scatterer contained in the far field operator for the whole ensemble. As in [22], the *a priori* information on the position of the single scatterer allows for a sparse representation of the associated far field operator component that we aim to recover. Moreover, we will show that the remaining part of the far field operator can be approximated by a low-rank operator, which however is not sparse. Accordingly, the inverse problem is equivalent to recovering a sparse operator given the sum of this sparse operator with a low-rank operator plus some modeling error and possibly some data error. We show that a convex program called principal component pursuit (see [7, 8, 44]) can be applied for this purpose, and we establish necessary and sufficient conditions for unique solvability as well as stability estimates in the context of far field operator splitting.

Previous investigations of far field splitting based on suitable sparse representations of far field patterns have mainly been concentrated on source problems or scattering problems with a single incident wave. However, the basic reasoning developed in [20, 23, 24, 25, 26] is closely related to the perspective taken in the present work. Other approaches to wave splitting for time-harmonic inverse source problems have been proposed in [3, 39]. Furthermore, splitting problems for time-dependent scattering problems have been considered in [2, 19, 28].

The remainder of this article proceeds as follows. In Section 2 we briefly outline the theoretical background on the scattering problem and discuss sparsity and low-rank properties of far field operators. Then, in Section 3, we describe how principal component pursuit can be used to approximate solutions to the splitting problem considered in the paper, and we analyze the stability of this approach. Numerical results are given in Section 4, and we finally close with some conclusions.

2 Inhomogeneous medium scattering

Before we discuss sparsity and low-rank properties of far field operators associated to ensembles of compactly supported scatterers, we summarize some facts and basic notations concerning the direct scattering problem. We consider time-harmonic scattering from penetrable scatterers modeled by the Helmholtz equation in $\mathbb{R}^2$. Let $k > 0$ denote the wave number and $n^2 = 1 + q$ the index of refraction for a real-valued compactly supported contrast function $q \in L^\infty(\mathbb{R}^2)$ satisfying $q > -1$ a.e. in $\mathbb{R}^2$ and $q = 0$ a.e. in $\mathbb{R}^2 \setminus D$ for some bounded open subset $D \subseteq \mathbb{R}^2$. We call D the support of the scatterers and below we will assume D to be the union of a few

well-separated connected components.

Suppose the scatterers are illuminated by an incident plane wave

$$u^i(\boldsymbol{x}; \boldsymbol{d}) := \mathrm{e}^{\mathrm{i}k\boldsymbol{x}\cdot\boldsymbol{d}}, \qquad \boldsymbol{x} \in \mathbb{R}^2, \tag{2.1a}$$

along the illumination direction $\boldsymbol{d} \in S^1$. Then the total field $u_q \in H^1_{\mathrm{loc}}(\mathbb{R}^2)$ and the associated scattered field $u^s_q = u_q - u^i$ solves the Helmholtz equation

$$\Delta u_q + k^2 n^2 u_q = 0 \qquad \text{in } \mathbb{R}^2, \tag{2.1b}$$

together with the Sommerfeld radiation condition

$$\lim_{r\to\infty} \sqrt{r}\Big(\frac{\partial u^s_q}{\partial r}(\boldsymbol{x}; \boldsymbol{d}) - \mathrm{i}k u^s_q(\boldsymbol{x}; \boldsymbol{d})\Big) = 0, \qquad r = |\boldsymbol{x}| \to \infty, \tag{2.1c}$$

uniformly with respect to all directions $\boldsymbol{x}/|\boldsymbol{x}| \in S^1$. We often indicate dependencies on the illumination direction $\boldsymbol{d}$ by a second argument and dependencies on the contrast q by a subscript.

The unique weak solution $u_q \in H^1_{\mathrm{loc}}(\mathbb{R}^2)$ of (2.1) (see, e.g., [32, Thm. 7.13]) exhibits an asymptotic expansion as an outgoing cylindrical wave

$$u^s_q(\boldsymbol{x}; \boldsymbol{d}) = \frac{\mathrm{e}^{\mathrm{i}\pi/4}}{\sqrt{8\pi}} \frac{\mathrm{e}^{\mathrm{i}k|\boldsymbol{x}|}}{\sqrt{k|\boldsymbol{x}|}} u^\infty_q(\widehat{\boldsymbol{x}}; \boldsymbol{d}) + O\big(|\boldsymbol{x}|^{-\frac{3}{2}}\big), \qquad |\boldsymbol{x}| \to \infty,$$

uniformly in all observation directions $\widehat{\boldsymbol{x}} = \boldsymbol{x}/|\boldsymbol{x}| \in S^1$ (see, e.g., [32, Thm. 7.15]). Here, the far field pattern $u^\infty_q \in L^2(S^1 \times S^1)$ is given by

$$u^\infty_q(\widehat{\boldsymbol{x}}; \boldsymbol{d}) = k^2 \int_D q(\boldsymbol{y}) u_q(\boldsymbol{y}; \boldsymbol{d}) \mathrm{e}^{-\mathrm{i}k\widehat{\boldsymbol{x}}\cdot\boldsymbol{y}} \, \mathrm{d}\boldsymbol{y}, \qquad \widehat{\boldsymbol{x}} \in S^1. \tag{2.2}$$

Accordingly, the far field operator

$$F_q : L^2(S^1) \to L^2(S^1), \quad (F_q g)(\widehat{\boldsymbol{x}}) := \int_{S^1} u^\infty_q(\widehat{\boldsymbol{x}}; \boldsymbol{d}) g(\boldsymbol{d}) \, \mathrm{d}s(\boldsymbol{d}), \tag{2.3}$$

which is determined by the far field patterns $u^\infty_q(\widehat{\boldsymbol{x}}; \boldsymbol{d})$ for all possible observation and incident directions $\widehat{\boldsymbol{x}}, \boldsymbol{d} \in S^1$, is often considered as an idealized measurement operator for remote sensing experiments in inverse scattering theory. This operator is well-known to be compact and normal (see, e.g., [32, Thm. 7.20]), and it is of trace class (see [12]) and thus in particular a Hilbert–Schmidt operator. For later reference we denote the space of Hilbert–Schmidt operators on $L^2(S^1)$ by $\mathrm{HS}(L^2(S^1))$.

2.1 Far field operator splitting

To simplify the presentation we restrict the discussion in the following to ensembles of two scatterers. Accordingly, we assume that the scatterer $D = D_1 \cup D_2$ consists of two well-separated components $D_1, D_2 \subseteq \mathbb{R}^2$ such that $D_j \subseteq B_{R_j}(\boldsymbol{c}_j)$, $j = 1, 2$, for some $R_1, R_2 > 0$ and $\boldsymbol{c}_1, \boldsymbol{c}_2 \in \mathbb{R}^2$ satisfying $|\boldsymbol{c}_1 - \boldsymbol{c}_2| > R_1 + R_2$, and we denote $q_1 := q|_{D_1}$ and $q_2 := q|_{D_2}$. However, we note that our analysis immediately extends to the case when $D \setminus D_1$ consists of more than one component.

Let us first recap the far field operator splitting problem as considered in [22]. Given the far field operator F_q, the wave number k and sufficient *a priori* information on the location of D_1 and D_2 (i.e., about $\boldsymbol{c}_1$ and $\boldsymbol{c}_2$) the goal in [22] was to recover the far field operators F_{q_1} and F_{q_2} corresponding to the two individual components of the scatterer. The procedure in [22] is based on splitting the given data into three parts,

$$F_q = F_{q_1} + F_{q_2} + F_{q_1,q_2},$$

3

and approximating each of these three components by sparse operators with respect to certain suitably modulated Fourier bases of $L^2(S^1)$. In this decomposition $F_{q_1,q_2} = F_q - (F_{q_1} + F_{q_2})$ represents those multiple scattering components that involve scattering both on q_1 and q_2 and therefore can neither be assigned to F_{q_1} nor to F_{q_2}. Accordingly, F_{q_1,q_2} is the part of F_q that has to be removed when recovering F_{q_1} and F_{q_2}.

In this paper, we consider a modified version of this far field operator splitting problem. We assume that only *a priori* information on the approximate location of D_1 (i.e., about c_1) is available, and we are only interested in recovering the far field operator F_{q_1} associated to the first component of the scatterer. Accordingly, we split the given far field data

$$F_q = F_{q_1} + F_{q \setminus q_1}$$

into two parts. Our strategy remains to approximate F_{q_1} by a sparse operator with respect to the same modulated Fourier basis as before. However, in contrast to [22], we now approximate the remaining part $F_{q \setminus q_1}$ by an operator of low-rank, which does not require any *a priori* information on the approximate location of D_2 (i.e., about c_2).

2.2 Sparse and low-rank approximations of far field operators

If $u_q \in H^1_{\mathrm{loc}}(\mathbb{R}^2)$ is the solution to the scattering problem (2.1), then $u_q|_D \in L^2(D)$ satisfies the Lippmann–Schwinger integral equation

$$u_q(\boldsymbol{x}; \boldsymbol{d}) = u^i(\boldsymbol{x}; \boldsymbol{d}) + k^2 \int_{\mathbb{R}^2} q(\boldsymbol{y}) \Phi(\boldsymbol{x} - \boldsymbol{y}) u_q(\boldsymbol{y}; \boldsymbol{d}) \, \mathrm{d}\boldsymbol{y}, \qquad \boldsymbol{x} \in D \,.$$

Here, $\Phi(\boldsymbol{x}) := \frac{\mathrm{i}}{4} H_0^{(1)}(k|\boldsymbol{x}|)$, $\boldsymbol{x} \neq \boldsymbol{0}$, denotes the fundamental solution to the Helmholtz equation (cf., e.g., [32, Thm. 7.12]). Introducing $L_q : L^2(D) \to L^2(D)$ by

$$(L_q f)(\boldsymbol{x}) := k^2 \int_D q(\boldsymbol{y}) f(\boldsymbol{y}) \Phi(\boldsymbol{x} - \boldsymbol{y}) \, \mathrm{d}\boldsymbol{y}, \qquad \boldsymbol{x} \in D \,,$$

yields the Born series representation

$$u_q^s(\,\cdot\,; \boldsymbol{d}) = \sum_{l=1}^{\infty} (L_q)^l u^i(\,\cdot\,; \boldsymbol{d}) \qquad \text{in } \mathbb{R}^2 \,, \tag{2.4}$$

of the scattered field, provided that the operator norm $\|L_q\|$ is strictly less than one (see, e.g., [29, 31, 37, 41, 42] for more detailed discussions). Neglecting terms of order $l \geq 3$ in (2.4) (i.e., considering the second order Born approximation) and substituting the result into (2.2) and (2.3), it has been established in [22] that the far field operator can be approximated in terms of

$$F_q \approx F_1 + F_2 + (F_{1,2} + F_{2,1}), \tag{2.5}$$

where $F_1 \approx F_{q_1}$ and $F_2 \approx F_{q_1}$ denote the second order Born approximations of the far field operators F_{q_1} and F_{q_2} associated to the two components of the scatterer in D_1 and D_2, respectively, and $F_{1,2} + F_{2,1} \approx F_q - F_{q_1} - F_{q_2}$ is the second order Born approximation of the remaining multiple scattering effects.

Denoting by $(\boldsymbol{e}_n)_n := (\mathrm{e}^{\mathrm{i} n \arg(\,\cdot\,)}/\sqrt{2\pi})_n$ the standard Fourier basis of $L^2(S^1)$, and introducing the far field translation operator

$$T_{\boldsymbol{c}_j} : L^2(S^1) \to L^2(S^1), \quad (T_{\boldsymbol{c}_j} g)(\widehat{\boldsymbol{x}}) := \mathrm{e}^{\mathrm{i} k \boldsymbol{c}_j \cdot \widehat{\boldsymbol{x}}} g(\widehat{\boldsymbol{x}}), \tag{2.6}$$

Figure 2.1: Left: Support of two scatterers D_1, D_2 (solid) contained in discs $B_{R_1}(\boldsymbol{c}_1)$, $B_{R_2}(\boldsymbol{c}_2)$ (dashed). Center and right: Absolute values of modulated Fourier coefficients $(a_{m,n})_{m,n}$ of far field operator components F_{q_1} (center) and $F_{q\setminus q_1}$ (right) at wave number $k = 1$. Dashed square (center) and dashed cross (right) correspond to active coefficients in sparse approximation of F_{q_1} in $\mathcal{V}_{N_1}^{\boldsymbol{c}_1}$ with $N_1 = 7$ and to those in low-rank approximation of $F_{q\setminus q_1}$ in $\mathcal{W}_{N_2}^{\boldsymbol{c}_2}$ with $N_2 = 7$, respectively.

we define the finite dimensional subspaces $\mathcal{V}_{N_j,N_l}^{\boldsymbol{c}_j,\boldsymbol{c}_l} \subseteq \mathrm{HS}(L^2(S^1))$ for all possible combinations of $j,l \in \{1,2\}$ by

$$\mathcal{V}_{N_j,N_l}^{\boldsymbol{c}_j,\boldsymbol{c}_l} := \left\{ G \in \mathrm{HS}(L^2(S^1)) \,\Big|\, Gg = \sum_{|m|\leq N_j} \sum_{|n|\leq N_l} a_{m,n}\, T_{-\boldsymbol{c}_j}\boldsymbol{e}_m \langle g, T_{-\boldsymbol{c}_l}\boldsymbol{e}_n \rangle_{L^2(S^1)},\ a_{m,n} \in \mathbb{C} \right\}. \tag{2.7}$$

We also use the short hand $\mathcal{V}_{N_j}^{\boldsymbol{c}_j} := \mathcal{V}_{N_j,N_j}^{\boldsymbol{c}_j,\boldsymbol{c}_j}$, $j = 1,2$. One of the main outcomes of [22] has been that the far field operator components F_1, F_2, $F_{1,2}$, and $F_{2,1}$ in the second order Born approximation (2.5) of the far field operator F_q can be well approximated in $\mathcal{V}_{N_1}^{\boldsymbol{c}_1}$, $\mathcal{V}_{N_2}^{\boldsymbol{c}_2}$, $\mathcal{V}_{N_1,N_2}^{\boldsymbol{c}_1,\boldsymbol{c}_2}$, and $\mathcal{V}_{N_2,N_1}^{\boldsymbol{c}_2,\boldsymbol{c}_1}$, respectively, whenever we choose $N_1 \gtrsim kR_1$ and $N_2 \gtrsim kR_2$. Here the notation $\gtrsim$ means "somewhat larger". Corresponding approximation error estimates have been provided in [22, Lmm. 3.4].

For moderate values of $N_1 \in \mathbb{N}$ the approximation of F_1 in $\mathcal{V}_{N_1}^{\boldsymbol{c}_1}$ as in (2.7) can be considered to be sparse, because it involves at most $(2N_1+1)^2$ nonzero coefficients. Defining another finite dimensional subspace $\mathcal{W}_{N_2}^{\boldsymbol{c}_2} \subseteq \mathrm{HS}(L^2(S^1))$ by

$$\mathcal{W}_{N_2}^{\boldsymbol{c}_2} := \Big\{ G \in \mathrm{HS}(L^2(S^1)) \,\Big|\, Gg = \sum_{|n|\leq N_2} \Big(T_{-\boldsymbol{c}_2}\boldsymbol{e}_n \langle g, \alpha_n \rangle_{L^2(S^1)}$$
$$+ \beta_n \langle g, T_{-\boldsymbol{c}_2}\boldsymbol{e}_n \rangle_{L^2(S^1)} \Big),\ \alpha_n, \beta_n \in L^2(S^1) \Big\}, \tag{2.8}$$

we immediately observe that $\mathcal{V}_{N_j,N_l}^{\boldsymbol{c}_j,\boldsymbol{c}_l} \subseteq \mathcal{W}_{N_2}^{\boldsymbol{c}_2}$ whenever $j = 2$ or $l = 2$. Consequently, the sum of operators $F_2 + F_{1,2} + F_{2,1}$ can be well approximated in $\mathcal{W}_{N_2}^{\boldsymbol{c}_2}$. Since

$$\mathrm{rank}\, G \leq 2(2N_2 + 1) \qquad \text{for any } G \in \mathcal{W}_{N_2}^{\boldsymbol{c}_2},$$

this implies that for moderate values of $N_2 \in \mathbb{N}$ the approximation of $F_2 + F_{1,2} + F_{2,1}$ in $\mathcal{W}_{N_2}^{\boldsymbol{c}_2}$ as in (2.8) is low-rank.

To sum up, the idea in the following is to compute a sparse operator $F_1 \in \mathcal{V}_{N_1}^{\boldsymbol{c}_1}$ and a low-rank operator $L \in \mathcal{W}_{N_2}^{\boldsymbol{c}_2}$ such that

$$F_q \approx F_1 + L \tag{2.9}$$

and to approximate F_{q_1} by F_1 and $F_{q\setminus q_1} = F_q - F_{q_1}$ by L.

Example 2.1. We illustrate the essential supports of the modulated Fourier coefficients of F_{q_1} and $F_{q\backslash q_1}$ by a numerical example with $q = \chi_{D_1} - 0.5\chi_{D_2}$ for D_1 and D_2 as shown in Figure 2.1 (left). Using a Nyström method (see, e.g., [13, pp. 91–96]) for the associated transmission problem, we simulate the far field patterns $u_q^\infty(\widehat{\boldsymbol{x}}_m; \boldsymbol{d}_n)$ and $u_{q_1}^\infty(\widehat{\boldsymbol{x}}_m; \boldsymbol{d}_n)$ for $M = 170$ equidistant observation and illumination directions on S^1 at wave number $k = 1$. The matrices

$$\boldsymbol{F}_{q_1} := \frac{2\pi}{M}[u_{q_1}^\infty(\widehat{\boldsymbol{x}}_m; \boldsymbol{d}_n)]_{1\le m,n\le M} \quad \text{and} \quad \boldsymbol{F}_{q\backslash q_1} := \frac{2\pi}{M}[u_q^\infty(\widehat{\boldsymbol{x}}_m; \boldsymbol{d}_n) - u_{q_1}^\infty(\widehat{\boldsymbol{x}}_m; \boldsymbol{d}_n)]_{1\le m,n\le M}$$

then approximate the far field operator components F_{q_1} and $F_{q\backslash q_1}$. The dashed discs in Figure 2.1 (left) are centered at $\boldsymbol{c}_1 = (-28, -30)^\top$ and $\boldsymbol{c}_2 = (26, -3)^\top$ with radii $R_1 = R_2 = 5$, respectively. Taking the two-dimensional Fourier transform of $\boldsymbol{F}_{q_1}$ and $\boldsymbol{F}_{q\backslash q_1}$ after multiplication with the appropriate modulation factors yields an approximation of the modulated Fourier coefficients $(a_{m,n})_{m,n}$ of F_{q_1} in terms of $(T_{-\boldsymbol{c}_1}\boldsymbol{e}_n)_n$ and of $F_{q\backslash q_1}$ in terms of $(T_{-\boldsymbol{c}_2}\boldsymbol{e}_n)_n$, respectively. In Figure 2.1 (center, right) the absolute values of these modulated Fourier coefficients are plotted using a logarithmic color scale. In the plot in the center, it can be observed that they are essentially supported in a square $[-N_1, N_1]^2$ for $N_1 = 7 \gtrsim 5 = kR_1$. In the right plot, the coefficients with the largest magnitude are essentially supported in the cross-shaped index set $\{(m, n) : |m| \le N_2 \text{ or } |n| \le N_2\}$ for $N_2 = 7 \gtrsim 5 = kR_2$. However, the contribution of the coefficients outside the cross-shaped index set is larger than in the middle plot, which leads to a larger approximation error for the projection of $F_{q\backslash q_1}$ onto $\mathcal{W}_{N_2}^{\boldsymbol{c}_2}$ compared to the projection of F_{q_1} onto $\mathcal{V}_{N_1}^{\boldsymbol{c}_1}$. This is caused by those far field operator components of scattering order three or higher, that can actually be approximated well in $\mathcal{V}_{N_1}^{\boldsymbol{c}_1}$, but belong to $F_{q\backslash q_1}$ and not to F_{q_1}. ◇

The splitting ansatz in (2.9) will only work reliably if we can ensure that the low-rank operators in $\mathcal{W}_{N_2}^{\boldsymbol{c}_2}$ do not have a sparse representation in $\mathcal{V}_{N_1}^{\boldsymbol{c}_1}$. The following section addresses this question.

2.3 When does sparse plus low-rank far field operator splitting work?

To avoid cluttered notation we write $\mathcal{V} := \mathcal{V}_{N_1}^{\boldsymbol{c}_1}$ and $\mathcal{W} := \mathcal{W}_{N_2}^{\boldsymbol{c}_2}$ in the following. We denote the orthogonal projections onto $\mathcal{V}$ and $\mathcal{W}$ by $\mathcal{P}_\mathcal{V}$ and $\mathcal{P}_\mathcal{W}$, respectively, and we define $\mathcal{P}_{\mathcal{V}^\perp} := \mathcal{I} - \mathcal{P}_\mathcal{V}$ and $\mathcal{P}_{\mathcal{W}^\perp} := \mathcal{I} - \mathcal{P}_\mathcal{W}$.

Operators $G = G_1 + G_2 \in \mathcal{V} + \mathcal{W}$ can be uniquely decomposed into $G_1 \in \mathcal{V}$ and $G_2 \in \mathcal{W}$ if and only if $\mathcal{V} \cap \mathcal{W} = \{0\}$. This is the case if and only if the cosine of the minimal angle between $\mathcal{V}$ and $\mathcal{W}$,

$$\|\mathcal{P}_\mathcal{V}\mathcal{P}_\mathcal{W}\| = \sup_{G\in\mathcal{V},\, H\in\mathcal{W}} \frac{|\langle G, H\rangle_{\mathrm{HS}}|}{\|G\|_{\mathrm{HS}}\|H\|_{\mathrm{HS}}}, \tag{2.10}$$

is strictly smaller than one (cf., e.g., [15, Lmm. 2.10]). Moreover, the smaller $\|\mathcal{P}_\mathcal{V}\mathcal{P}_\mathcal{W}\|$ is, the more robust splitting becomes with respect to noise in the data G. Thus, the aim of this section is to develop an upper bound for $\|\mathcal{P}_\mathcal{V}\mathcal{P}_\mathcal{W}\|$, similar to what has been established in [22, Props. 3.8 and 3.14]. We start with some additional notations and technical remarks.

Remark 2.2. Apart from the usual Hilbert–Schmidt norm, we will also use some other norms on $\mathrm{HS}(L^2(S^1))$ in our analysis below. We first recall that any operator $G \in \mathrm{HS}(L^2(S^1))$ can be expanded in terms of the Fourier basis $(\boldsymbol{e}_n)_n \subseteq L^2(S^1)$ via

$$Gf = \sum_{m\in\mathbb{Z}}\sum_{n\in\mathbb{Z}} a_{m,n}\, \boldsymbol{e}_m\langle f, \boldsymbol{e}_n\rangle_{L^2(S^1)}, \qquad g \in L^2(S^1), \tag{2.11}$$

with Fourier coefficients $(a_{m,n})_{m,n} = (\langle G\boldsymbol{e}_n, \boldsymbol{e}_m\rangle_{L^2(S^1)})_{m,n} \in \ell^2 \times \ell^2$. For $1 \le p \le \infty$ this representation gives rise to the norms

$$\|G\|_{\ell^p\times\ell^p} := \|(a_{m,n})_{m,n}\|_{\ell^p\times\ell^p}, \qquad G \in \mathrm{HS}(L^2(S^1)),$$

at least if the right hand side is finite. On the other hand, $G \in \mathrm{HS}(L^2(S^1))$ also possesses a singular value decomposition

$$Gf = \sum_{n \in \mathbb{N}} \sigma_n\, u_n \langle f, v_n \rangle_{L^2(S^1)}, \qquad f \in L^2(S^1),$$

with singular values $(\sigma_n)_n \in \ell^2$ and singular vectors $(u_n)_n, (v_n)_n \subseteq L^2(S^1)$. Therewith the Hilbert–Schmidt norm of an operator G can be written as $\|G\|_{\mathrm{HS}} = \|(\sigma_n)_n\|_{\ell^2}$, its nuclear norm as $\|G\|_{\mathrm{nuc}} = \|(\sigma_n)_n\|_{\ell^1}$ and its operator norm as $\|G\| = \|(\sigma_n)_n\|_{\ell^\infty}$. Furthermore, Parseval's identity shows that

$$\langle G, H \rangle_{\mathrm{HS}} = \langle G, H \rangle_{\ell^2 \times \ell^2} \qquad \text{for } G, H \in \mathrm{HS}(L^2(S^1)).$$

We also denote the number of nonzero coefficients $(a_{m,n})_{m,n}$ in (2.11) by $\|G\|_{\ell^0 \times \ell^0}$ and we recall that the number of nonzero singular values $(\sigma_n)_n$ of G coincides with $\mathrm{rank}(G)$. $\quad\diamond$

To relate the modulated Fourier bases in the definitions (2.7) of $\mathcal{V}$ and (2.8) of $\mathcal{W}$ to the unmodulated Fourier basis $(e_n)_n$, we introduce for any $\boldsymbol{c} \in \mathbb{R}^2$ the operator

$$\boldsymbol{\mathcal{T}_c} : \mathrm{HS}(L^2(S^1)) \to \mathrm{HS}(L^2(S^1)), \quad \boldsymbol{\mathcal{T}_c} G := T_{\boldsymbol{c}} \circ G \circ T_{-\boldsymbol{c}}, \tag{2.12}$$

where $T_{\boldsymbol{c}}$ has already been defined in (2.6). The mapping properties of $\boldsymbol{\mathcal{T}_c}$ have proven to be an essential tool in [22]. To begin with, we note that $F_{q_j(\cdot + \boldsymbol{c}_j)} = \boldsymbol{\mathcal{T}_{c_j}} F_{q_j}$ for $j = 1, 2$, and accordingly the subspaces $\mathcal{V}$ and $\mathcal{W}$ can be rewritten as

$$\mathcal{V} = \left\{ G \in \mathrm{HS}(L^2(S^1)) \,\middle|\, \boldsymbol{\mathcal{T}_{c_1}} G \in \mathcal{V}_{N_1}^{\boldsymbol{0}} \right\} \quad \text{and} \quad \mathcal{W} = \left\{ G \in \mathrm{HS}(L^2(S^1)) \,\middle|\, \boldsymbol{\mathcal{T}_{c_2}} G \in \mathcal{W}_{N_2}^{\boldsymbol{0}} \right\}.$$

The following lemma presents further results that are relevant for this work.

Lemma 2.3. *Let $\boldsymbol{c} \in \mathbb{R}^2$ with $\boldsymbol{c} \neq \boldsymbol{0}$. Then,*
(a) $\boldsymbol{\mathcal{T}_c}$ is a unitary operator on $\mathrm{HS}(L^2(S^1))$ with $\boldsymbol{\mathcal{T}_c}^* = \boldsymbol{\mathcal{T}_{-c}}$,
(b) $\boldsymbol{\mathcal{T}_c}$ preserves the norms $\|\cdot\|_{\mathrm{HS}}, \|\cdot\|_{\mathrm{nuc}}$ and $\|\cdot\|$ as well as the rank, and
(c) for any $\boldsymbol{c} \in \mathbb{R}^2$ and $N \in \mathbb{N}$, we have that

$$\|\boldsymbol{\mathcal{T}_c} G\|_{\ell^\infty \times \ell^\infty} \leq 2\beta_N^{\boldsymbol{c}} \|G\|_{\mathrm{HS}}, \qquad G \in \mathcal{W}_N^{\boldsymbol{0}}, \tag{2.13}$$

where

$$\beta_N^{\boldsymbol{c}} := \sqrt{\sup_{n \in \mathbb{Z}} \left(\sum_{|n'-n| \leq N} J_{n'}^2(k|\boldsymbol{c}|) \right)} \leq \min\left\{ 1, b\sqrt{\frac{2N+1}{k|\boldsymbol{c}|}} \right\} \tag{2.14}$$

with $b \approx 0.7595$.

Proof. Part (a) follows immediately from the definitions (2.6) and (2.12) of $T_{\boldsymbol{c}}$ and $\boldsymbol{\mathcal{T}_c}$ (see [22, Lmm. 2.2]).

Since applying the unitary operator $\boldsymbol{\mathcal{T}_c}$ does not change the singular values of an operator $G \in \mathrm{HS}(L^2(S^1))$, part (b) follows from the characterizations of $\|\cdot\|_{\mathrm{HS}}, \|\cdot\|_{\mathrm{nuc}}$ and $\|\cdot\|$ in terms of the singular values at the end of Remark 2.2.

Part (c) requires a bit more effort. By definition (2.8) of $\mathcal{W}_N^{\boldsymbol{0}}$ and since

$$\left\{ (m', n') \,\middle|\, |m'| \leq N \text{ or } |n'| \leq N \right\}$$
$$= \left\{ (m', n') \,\middle|\, m' \in \mathbb{Z}, |n'| \leq N \right\} \cup \left\{ (m', n') \,\middle|\, |m'| \leq N, |n'| > N \right\},$$

we can write any $G \in \mathcal{W}_N^{\mathbf{0}}$ as

$$G = \sum_{m' \in \mathbb{Z}} \sum_{|n'| \leq N} a_{m',n'} \, \boldsymbol{e}_{m'} \langle \, \cdot \, , \boldsymbol{e}_{n'} \rangle_{L^2(S^1)} + \sum_{|m'| \leq N} \sum_{|n'| > N} a_{m',n'} \, \boldsymbol{e}_{m'} \langle \, \cdot \, , \boldsymbol{e}_{n'} \rangle_{L^2(S^1)} \, .$$

We conclude by expanding $T_{\boldsymbol{c}} \boldsymbol{e}_{m'}$ in terms of $(\boldsymbol{e}_m)_m$ and $T_{\boldsymbol{c}} \boldsymbol{e}_{n'}$ in terms of $(\boldsymbol{e}_n)_n$ that the coefficients $(a_{m,n}^{\boldsymbol{c}})_{m,n}$ in the Fourier expansion of $\boldsymbol{\mathcal{T}_c} G$ as in (2.11) are given by

$$a_{m,n}^{\boldsymbol{c}} = \sum_{m' \in \mathbb{Z}} \sum_{|n'| \leq N} a_{m',n'} \langle T_{\boldsymbol{c}} \boldsymbol{e}_{m'}, \boldsymbol{e}_m \rangle_{L^2(S^1)} \langle \boldsymbol{e}_n, T_{\boldsymbol{c}} \boldsymbol{e}_{n'} \rangle_{L^2(S^1)}$$

$$+ \sum_{|m'| \leq N} \sum_{|n'| > N} a_{m',n'} \langle T_{\boldsymbol{c}} \boldsymbol{e}_{m'}, \boldsymbol{e}_m \rangle_{L^2(S^1)} \langle \boldsymbol{e}_n, T_{\boldsymbol{c}} \boldsymbol{e}_{n'} \rangle_{L^2(S^1)}$$

for $m, n \in \mathbb{Z}$. Throughout this work, $\langle \, \cdot \, , \, \cdot \, \rangle_{L^2(S^1)}$ is linear in its first and antilinear in its second argument. Accordingly, applying the Cauchy–Schwarz inequality we deduce that

$$\|\boldsymbol{\mathcal{T}_c} G\|_{\ell^\infty \times \ell^\infty} = \|(a_{m,n}^{\boldsymbol{c}})_{m,n}\|_{\ell^\infty \times \ell^\infty}$$

$$\leq 2 \sqrt{\sup_{m \in \mathbb{Z}} \left(\sum_{m' \in \mathbb{Z}} |\langle T_{\boldsymbol{c}} \boldsymbol{e}_{m'}, \boldsymbol{e}_m \rangle_{L^2(S^1)}|^2 \right) \sup_{n \in \mathbb{Z}} \left(\sum_{|n'| \leq N} |\langle T_{\boldsymbol{c}} \boldsymbol{e}_{n'}, \boldsymbol{e}_n \rangle_{L^2(S^1)}|^2 \right)} \|G\|_{\mathrm{HS}} = 2 \beta_N^{\boldsymbol{c}} \|G\|_{\mathrm{HS}} \, .$$

For the last equality, we used that $|\langle T_{\boldsymbol{c}} \boldsymbol{e}_{n'}, \boldsymbol{e}_n \rangle_{L^2(S^1)}|^2 = J_{n-n'}^2(k|\boldsymbol{c}|)$ due to the Jacobi–Anger expansion

$$\mathrm{e}^{\pm \mathrm{i} k \widehat{\boldsymbol{x}} \cdot \boldsymbol{y}} = \sum_{n \in \mathbb{Z}} (\pm \mathrm{i})^n \mathrm{e}^{-\mathrm{i} n \arg \boldsymbol{y}} J_n(k|\boldsymbol{y}|) \mathrm{e}^{\mathrm{i} n \arg \widehat{\boldsymbol{x}}} \, , \qquad \boldsymbol{y} \in \mathbb{R}^2 \, , \ \widehat{\boldsymbol{x}} \in S^1 \, , \tag{2.15}$$

and that $\|(J_m(k|\boldsymbol{c}|))_m\|_{\ell^2} = 1$ (see, e.g., [16, Eq. (10.23.3)]). Applying the uniform upper bound for the Bessel functions from [34, Thm. 2] finally gives the second inequality in (2.14). $\qquad \square$

Now we are ready to establish an upper bound for $\|\mathcal{P}_{\mathcal{V}} \mathcal{P}_{\mathcal{W}}\|$ from (2.10).

Proposition 2.4. *For all $G \in \mathcal{V}$ and $H \in \mathcal{W}$ we have that*

$$\frac{|\langle G, H \rangle_{\mathrm{HS}}|}{\|G\|_{\mathrm{HS}} \|H\|_{\mathrm{HS}}} \leq 2 \sqrt{\|\boldsymbol{\mathcal{T}}_{\boldsymbol{c}_1} G\|_{\ell^0 \times \ell^0}} \, \beta_{N_2}^{\boldsymbol{c}_1 - \boldsymbol{c}_2} \leq \frac{8(2N_1 + 1)\sqrt{2N_2 + 1}}{5\sqrt{k|\boldsymbol{c}_1 - \boldsymbol{c}_2|}} \, . \tag{2.16}$$

Proof. We use Lemma 2.3, Hölder's inequality and the inequality $\| \cdot \| \leq \| \cdot \|_{\mathrm{HS}}$ to estimate

$$|\langle G, H \rangle_{\mathrm{HS}}| = |\langle \boldsymbol{\mathcal{T}}_{\boldsymbol{c}_1} G, \boldsymbol{\mathcal{T}}_{\boldsymbol{c}_1 - \boldsymbol{c}_2}(\boldsymbol{\mathcal{T}}_{\boldsymbol{c}_2} H) \rangle_{\ell^2 \times \ell^2}| \leq \|\boldsymbol{\mathcal{T}}_{\boldsymbol{c}_1} G\|_{\ell^1 \times \ell^1} \|\boldsymbol{\mathcal{T}}_{\boldsymbol{c}_1 - \boldsymbol{c}_2}(\boldsymbol{\mathcal{T}}_{\boldsymbol{c}_2} H)\|_{\ell^\infty \times \ell^\infty}$$

$$\leq 2 \sqrt{\|\boldsymbol{\mathcal{T}}_{\boldsymbol{c}_1} G\|_{\ell^0 \times \ell^0}} \, \beta_{N_2}^{\boldsymbol{c}_1 - \boldsymbol{c}_2} \|\boldsymbol{\mathcal{T}}_{\boldsymbol{c}_1} G\|_{\mathrm{HS}} \|\boldsymbol{\mathcal{T}}_{\boldsymbol{c}_2} H\|_{\mathrm{HS}} = 2 \sqrt{\|\boldsymbol{\mathcal{T}}_{\boldsymbol{c}_1} G\|_{\ell^0 \times \ell^0}} \, \beta_{N_2}^{\boldsymbol{c}_1 - \boldsymbol{c}_2} \|G\|_{\mathrm{HS}} \|H\|_{\mathrm{HS}} \, .$$

Recalling that $\|\boldsymbol{\mathcal{T}}_{\boldsymbol{c}_1} G\|_{\ell^0 \times \ell^0} \leq (2N_1 + 1)^2$ for any $G \in \mathcal{V}$, and using the upper bound for $\beta_{N_2}^{\boldsymbol{c}_1 - \boldsymbol{c}_2}$ from (2.14) completes the proof. $\qquad \square$

Remark 2.5. Using the Jacobi–Anger expansion (2.15) we can rewrite

$$\beta_{N_2}^{\boldsymbol{c}_1 - \boldsymbol{c}_2} = \sqrt{\sup_{n \in \mathbb{Z}} \left(\sum_{|n'| \leq N_2} |\langle T_{-\boldsymbol{c}_2} \boldsymbol{e}_{n'}, T_{-\boldsymbol{c}_1} \boldsymbol{e}_n \rangle_{L^2(S^1)}|^2 \right)} \, .$$

This shows that $\beta_{N_2}^{\boldsymbol{c}_1 - \boldsymbol{c}_2}$ is a measure of incoherence of $\mathrm{span}\{T_{-\boldsymbol{c}_2} \boldsymbol{e}_{n'} \, : \, |n'| \leq N_2\} \subset L^2(S^1)$ with respect to the orthonormal system $\{T_{-\boldsymbol{c}_1} \boldsymbol{e}_n \, : \, n \in \mathbb{Z}\}$ in $L^2(S^1)$. If $\beta_{N_2}^{\boldsymbol{c}_1 - \boldsymbol{c}_2}$ is small, this
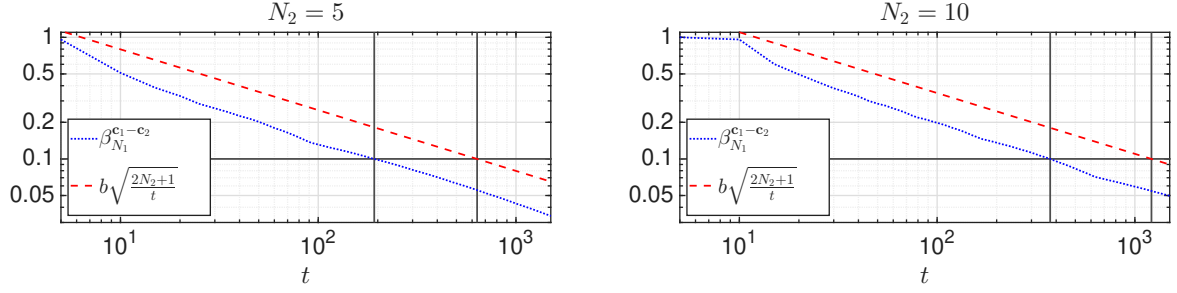
Figure 2.2: Plots of $\beta_{N_2}^{c_2-c_2}$ (dotted blue) and of the upper bound from (2.14) (dashed red) as function of $t = k|c_1 - c_2|$ on a double-logarithmic scale for $N_2 = 5$ (left) and for $N_2 = 10$ (right). The level 0.1 (solid gray) is attained by $\beta_{N_2}^{c_2-c_2}$ for $t > 191$ in the case $N_2 = 5$, and for $t > 372$ in the case $N_2 = 10$. The upper bound falls below the level 0.1 only for considerably larger values of t, namely for $t > 635$ when $N_2 = 5$ and for $t > 1212$ when $N_2 = 10$.

means that operators in $\mathcal{W}$ cannot have a sparse representation in $\mathcal{V}$. We note that $\beta_{N_2}^{c_1-c_2}$ corresponds to $\beta(S)$ as introduced in [8, Eq. (4.6)] for $S = \mathrm{span}\{T_{-c_2}e_{n'} : |n'| \leq N_2\}$ and the n-th standard basis vector replaced by $T_{-c_1}e_n$, $n \in \mathbb{Z}$. We also refer to [27], where a similar notion of incoherence was considered.

Our numerical results in Figure 2.2 suggest that the upper bound of $\beta_{N_2}^{c_1-c_2}$ in (2.14) is of optimal order but not sharp. To generate these plots, we have used the superlinear decay of $|J_m(t)|$ in $|m|$ for $|m| > |t|$, which ensures that the supremum in the definition of $\beta_{N_2}^{c_1-c_2}$ is already attained for moderate values of $n \in \mathbb{Z}$, to calculate $\beta_{N_2}^{c_1-c_2}$ numerically. However, the upper bound in (2.16) gives a good qualitative impression of sufficient conditions for the geometry of the scatterer to allow for stable splitting. The smaller the diameters of the two components are and the farther apart they are from each other, both in terms of the wave length, the smaller this bound becomes. Here, the size R_1 of the first scatterer has a stronger influence than R_2. ◇

In the next section we examine a convex program called principal component pursuit to approximate F_{q_1} based on *a priori* knowledge of c_1.

3 Far field operator splitting by principal component pursuit

Suppose that (F_1, L) is an approximate split of the far field operator F_q as in (2.9) such that $F_1 \in \mathcal{V}$ is sparse and $L \in \mathcal{W}$ is low-rank. Following [44] we consider the constrained optimization problem

$$\min_{\widetilde{F}_1, \widetilde{L} \in \mathrm{HS}(L^2(S^1))} \lambda\|\mathcal{T}_{c_1}\widetilde{F}_1\|_{\ell^1 \times \ell^1} + \|\widetilde{L}\|_{\mathrm{nuc}} \qquad \text{subject to} \qquad \|F_q^\delta - \widetilde{F}_1 - \widetilde{L}\|_{\mathrm{HS}} \leq \delta, \qquad (3.1)$$

to recover an approximation of (F_1, L) from possibly noisy observations $F_q^\delta \in \mathrm{HS}(L^2(S^1))$ of F_q. Here $\lambda \in (0, 1)$ is a coupling parameter that will be specified below. The parameter $\delta > 0$ not just accounts for the data error $F_q^\delta - F_q$ but also for the modeling error $F_q - F_1 - L$ that is caused by the sparse plus low-rank approximation according to (2.9).

Before we address the stable recovery of (F_1, L) by means of (3.1) in Theorem 3.5 below, we establish conditions on the diameters of the supports of the scatterers D_1 and D_2 and on their distance to each other in terms of the wave length that guarantee uniqueness of solutions to the unrelaxed optimization problem

$$\min_{\widetilde{F}_1, \widetilde{L} \in \mathrm{HS}(L^2(S^1))} \lambda\|\mathcal{T}_{c_1}\widetilde{F}_1\|_{\ell^1 \times \ell^1} + \|\widetilde{L}\|_{\mathrm{nuc}} \qquad \text{subject to} \qquad F_1 + L = \widetilde{F}_1 + \widetilde{L}. \qquad (3.2)$$

The latter is commonly referred to as Principal Component Pursuit (PCP). We note that in PCP the aim usually is to recover the low-rank matrix L – the principal component – while the sparse matrix component typically is of less interest. However, in our setting it is the other way round as our main goal is to recover the sparse component F_1.

For any $\widetilde{F}_1, \widetilde{L} \in \mathrm{HS}(L^2(S^1))$ we write

$$\Psi_\lambda(\widetilde{F}_1, \widetilde{L}) := \lambda \|\boldsymbol{\mathcal{T}}_{\boldsymbol{c}_1}\widetilde{F}_1\|_{\ell^1 \times \ell^1} + \|\widetilde{L}\|_{\mathrm{nuc}}. \tag{3.3}$$

A characterization of the subdifferential of Ψ_λ in (F_1, L) (see, e.g., [8, p. 580]) will be required in the proof of Proposition 3.1 below. Denoting the Fourier coefficients in the series representation of $\boldsymbol{\mathcal{T}}_{\boldsymbol{c}_1}F_1$ as in (2.11) by $(a_{m,n}^{\boldsymbol{c}_1})_{m,n}$ and by $(\sigma_n; u_n, v_n)_n$ a singular system for L, we introduce the two operators

$$\Sigma := \sum_{|m|\leq N_1} \sum_{|n|\leq N_1} \frac{\overline{a_{m,n}^{\boldsymbol{c}_1}}}{|a_{m,n}^{\boldsymbol{c}_1}|} T_{-\boldsymbol{c}_1}\boldsymbol{e}_m \langle \cdot, T_{-\boldsymbol{c}_1}\boldsymbol{e}_n\rangle_{L^2(S^1)} \quad \text{and} \quad \Lambda g := \sum_{n=1}^{2(2N_2+1)} u_n \langle \cdot, v_n\rangle_{L^2(S^1)}. \tag{3.4}$$

The following proposition is similar to [7, Lmm. 2.5] and [8, Prop. 2]. However, the translation operator $\boldsymbol{\mathcal{T}}_{\boldsymbol{c}_1}$ in (3.3) requires some subtle changes.

Proposition 3.1. *The pair (F_1, L) is the unique minimizer of* (3.2) *if*
(a) there holds $\|\mathcal{P}_{\mathcal{V}}\mathcal{P}_{\mathcal{W}}\| < 1/2$ and
(b) there exists a dual certificate $W \in \mathrm{HS}(L^2(S^1))$ satisfying

$$\mathcal{P}_{\mathcal{W}}W = 0, \quad \|W\| < \tfrac{1}{2}, \quad \|\mathcal{P}_{\mathcal{V}}(\Lambda - \lambda\Sigma + W)\|_{\mathrm{HS}} \leq \tfrac{\lambda}{4}, \quad \|\boldsymbol{\mathcal{T}}_{\boldsymbol{c}_1}\mathcal{P}_{\mathcal{V}^\perp}(\Lambda + W)\|_{\ell^\infty \times \ell^\infty} < \tfrac{\lambda}{4}. \tag{3.5}$$

Proof. Assume that the conditions (a) and (b) are satisfied. Since any feasible pair $(\widetilde{F}_1, \widetilde{L})$ for (3.2) can be written as $(F_1 - G, L + G)$ for some $G \in \mathrm{HS}(L^2(S^1))$, we have to show

$$\Psi_\lambda(F_1 - G, L + G) > \Psi_\lambda(F_1, L)$$

whenever $G \neq 0$. Let $Z_1 \in \partial\|\boldsymbol{\mathcal{T}}_{\boldsymbol{c}_1}F_1\|_{\ell^1 \times \ell^1}$ and $Z_L \in \partial\|L\|_{\mathrm{nuc}}$ be arbitrary subgradients, i.e.,

$$Z_1 = \Sigma + G_1 \quad \text{for some } G_1 \in \mathcal{V}^\perp \text{ with } \|\boldsymbol{\mathcal{T}}_{\boldsymbol{c}_1}G_1\|_{\ell^\infty \times \ell^\infty} \leq 1, \tag{3.6a}$$

$$Z_L = \Lambda + G_L \quad \text{for some } G_L \in \mathcal{W}^\perp \text{ with } \|G_L\| \leq 1. \tag{3.6b}$$

Then the subgradient property gives

$$\Psi_\lambda(F_1 - G, L + G) \geq \Psi_\lambda(F_1, L) - \lambda\langle Z_1, G\rangle_{\mathrm{HS}} + \langle Z_L, G\rangle_{\mathrm{HS}}. \tag{3.7}$$

We can choose G_1 and G_L satisfying (3.6) such that

$$\langle G_1, \mathcal{P}_{\mathcal{V}^\perp}G\rangle_{\mathrm{HS}} = -\|\boldsymbol{\mathcal{T}}_{\boldsymbol{c}_1}\mathcal{P}_{\mathcal{V}^\perp}G\|_{\ell^1 \times \ell^1} \quad \text{and} \quad \langle G_L, \mathcal{P}_{\mathcal{W}^\perp}G\rangle_{\mathrm{HS}} = \|\mathcal{P}_{\mathcal{W}^\perp}G\|_{\mathrm{nuc}}.$$

For G_1 this can be achieved by picking

$$G_1 = -\sum_{|m|>N_1} \sum_{|n|>N_1} \frac{\overline{b_{m,n}^{\boldsymbol{c}_1}}}{|b_{m,n}^{\boldsymbol{c}_1}|} T_{-\boldsymbol{c}_1}\boldsymbol{e}_n \langle \cdot, T_{-\boldsymbol{c}_1}\boldsymbol{e}_n\rangle_{L^2(S^1)}$$

with $(b_{m,n}^{\boldsymbol{c}_1})_{m,n}$ denoting the Fourier coefficients in the series representation of $\boldsymbol{\mathcal{T}}_{\boldsymbol{c}_1}G$ as in (2.11). The operator G_L can be constructed using the duality of $\|\cdot\|$ and $\|\cdot\|_{\mathrm{nuc}}$ as outlined in the proof of [7, Lmm. 2.5]. Inserting this into (3.7) we obtain

$$\Psi_\lambda(F_1 - G, L + G) \geq \Psi_\lambda(F_1, L) + \Psi_\lambda(\mathcal{P}_{\mathcal{V}^\perp}G, \mathcal{P}_{\mathcal{W}^\perp}G) - |\langle\lambda\Sigma - \Lambda, G\rangle_{\mathrm{HS}}|. \tag{3.8}$$

Rewriting $\Lambda - \lambda\Sigma = \mathcal{P}_{\mathcal{V}}(\Lambda - \lambda\Sigma + W) + \mathcal{P}_{\mathcal{V}^\perp}(\Lambda + W) - W$ and using Hölder's inequality as well as Lemma 2.3 (a)–(b) and the assumption (b) of the proposition, we can bound the third term on the right hand side of (3.8) by

$$
\begin{aligned}
|\langle \lambda\Sigma - \Lambda, G\rangle_{\mathrm{HS}}| &\leq |\langle \mathcal{P}_{\mathcal{V}}(\Lambda - \lambda\Sigma + W), G\rangle_{\mathrm{HS}}| + |\langle \mathcal{P}_{\mathcal{V}^\perp}(\Lambda + W), G\rangle_{\mathrm{HS}}| + |\langle W, G\rangle_{\mathrm{HS}}| \\
&\leq \tfrac{\lambda}{4}\|\mathcal{P}_{\mathcal{V}}G\|_{\mathrm{HS}} + \tfrac{\lambda}{4}\|\boldsymbol{\mathcal{T}}_{\boldsymbol{c}_1}\mathcal{P}_{\mathcal{V}^\perp}G\|_{\ell^1\times\ell^1} + \tfrac{1}{2}\|\mathcal{P}_{\mathcal{W}^\perp}G\|_{\mathrm{nuc}}\,.
\end{aligned} \tag{3.9}
$$

Using condition (a) of the proposition we conclude that

$$
\begin{aligned}
\|\mathcal{P}_{\mathcal{V}}G\|_{\mathrm{HS}} &\leq \|\mathcal{P}_{\mathcal{V}}\mathcal{P}_{\mathcal{W}}G\|_{\mathrm{HS}} + \|\mathcal{P}_{\mathcal{V}}\mathcal{P}_{\mathcal{W}^\perp}G\|_{\mathrm{HS}} \leq \tfrac{1}{2}\|G\|_{\mathrm{HS}} + \|\mathcal{P}_{\mathcal{W}^\perp}G\|_{\mathrm{HS}} \\
&= \tfrac{1}{2}\|\mathcal{P}_{\mathcal{V}}G\|_{\mathrm{HS}} + \tfrac{1}{2}\|\mathcal{P}_{\mathcal{V}^\perp}G\|_{\mathrm{HS}} + \|\mathcal{P}_{\mathcal{W}^\perp}G\|_{\mathrm{HS}}\,.
\end{aligned}
$$

Combining this with $\|\cdot\|_{\mathrm{HS}} \leq \|\cdot\|_{\ell^1\times\ell^1}$ and $\|\cdot\|_{\mathrm{HS}} \leq \|\cdot\|_{\mathrm{nuc}}$ we obtain that

$$
\|\mathcal{P}_{\mathcal{V}}G\|_{\mathrm{HS}} \leq \|\boldsymbol{\mathcal{T}}_{\boldsymbol{c}_1}\mathcal{P}_{\mathcal{V}^\perp}G\|_{\ell^1\times\ell^1} + 2\|\mathcal{P}_{\mathcal{W}^\perp}G\|_{\mathrm{nuc}}\,. \tag{3.10}
$$

Inserting (3.10) into (3.9) and the result into (3.8) finally yields

$$
\Psi_\lambda(F_1 - G, L + G) \geq \Psi_\lambda(F_1, L) + \tfrac{1}{2}\left(\lambda\|\boldsymbol{\mathcal{T}}_{\boldsymbol{c}_1}\mathcal{P}_{\mathcal{V}^\perp}G\|_{\ell^1\times\ell^1} + (1-\lambda)\|\mathcal{P}_{\mathcal{W}^\perp}G\|_{\mathrm{nuc}}\right)\,. \tag{3.11}
$$

The second term on the right hand side of (3.11) is nonnegative and vanishes if and only if $\mathcal{P}_{\mathcal{V}^\perp}G = \mathcal{P}_{\mathcal{W}^\perp}G = 0$, i.e., if and only if $G = 0$ as $\mathcal{V}\cap\mathcal{W} = \{0\}$ due to condition (a) of the proposition. This ends the proof. $\qquad\square$

In Proposition 3.3 below, we establish sufficient conditions on λ, k, N_1, N_2 and $|\boldsymbol{c}_1 - \boldsymbol{c}_2|$ such that the conditions (a) and (b) of Proposition 3.1 are fulfilled. For this purpose we define

$$
\mu := \sup_{G\in\mathcal{V},\,\|\boldsymbol{\mathcal{T}}_{\boldsymbol{c}_1}G\|_{\ell^\infty\times\ell^\infty}\leq 1}\|G\| \qquad\text{and}\qquad \xi := \sup_{G\in\mathcal{W},\,\|G\|\leq 1}\|\boldsymbol{\mathcal{T}}_{\boldsymbol{c}_1}G\|_{\ell^\infty\times\ell^\infty}\,,
$$

which correspond to $\mu(F_1)$ and $\xi(L)$ as introduced in [8, Eq. (1.1), (1.2)]. The number ξ being small means that for any $G \in \mathcal{W}$ the translated operator $\boldsymbol{\mathcal{T}}_{\boldsymbol{c}_1}G$ is not too sparse with respect to the Fourier basis $(\boldsymbol{e}_n)_n$. If the product of μ and ξ is sufficiently small, we can use arguments developed in [8] to establish uniqueness of the minimizer of (3.2). The following lemma expresses μ and ξ in terms of k, N_1, N_2 and $|\boldsymbol{c}_1 - \boldsymbol{c}_2|$.

Lemma 3.2. *There holds*

$$
\mu = 2N_1 + 1 \qquad\text{and}\qquad \xi \leq 2\beta_{N_2}^{\boldsymbol{c}_1-\boldsymbol{c}_2}
$$

with $\beta_{N_2}^{\boldsymbol{c}_1-\boldsymbol{c}_2}$ as in (2.14).

Proof. The upper bound for ξ follows immediately from (2.13).

For μ we conclude from Lemma 2.3 (b) and Parseval's identity for any $G \in \mathcal{V}$ with $(a_{m,n}^{\boldsymbol{c}_1})_{m,n}$ denoting the coefficients of the series expansion of $\boldsymbol{\mathcal{T}}_{\boldsymbol{c}_1}G$ as in (2.11) that

$$
\begin{aligned}
\|G\| = \|\boldsymbol{\mathcal{T}}_{\boldsymbol{c}_1}G\| &= \sup_{\|f\|_{L^2(S^1)}=1}\|(\boldsymbol{\mathcal{T}}_{\boldsymbol{c}_1}G)f\|_{L^2(S^1)} = \sup_{\|f\|_{L^2(S^1)}=1}\sqrt{\sum_{|m|\leq N_1}|\langle(\boldsymbol{\mathcal{T}}_{\boldsymbol{c}_1}G)f, \boldsymbol{e}_m\rangle|_{L^2(S^1)}^2} \\
&= \sup_{\|f\|_{L^2(S^1)}=1}\sqrt{\sum_{|m|\leq N_1}\left|\sum_{|n|\leq N_1}a_{m,n}^{\boldsymbol{c}_1}\langle f, \boldsymbol{e}_n\rangle_{L^2(S^1)}^2\right|} \leq (2N_1+1)\|\boldsymbol{\mathcal{T}}_{\boldsymbol{c}_1}G\|_{\ell^\infty\times\ell^\infty}\,.
\end{aligned}
$$

This yields $\mu \leq 2N_1+1$ and since the upper bound is attained for $f = \sum_{|m|\leq N_1}T_{-\boldsymbol{c}_1}\boldsymbol{e}_m/(2N_1+1)$, we obtain equality. $\qquad\square$

The following proposition adapts the sufficient conditions for uniqueness of minimizers established in [8, Thm. 2] for our far field operator splitting problem.

Proposition 3.3. *The conditions (a) and (b) of Proposition 3.1 are satisfied for*

$$\lambda \in \left(\frac{8\beta_{N_1}^{c_1-c_2}}{1 - 8(N_1 + 3)(2N_1 + 1)\beta_{N_1}^{c_1-c_2}}, \frac{2(1 - 16(2N_1 + 1)^2\beta_{N_1}^{c_1-c_2})}{15(2N_1 + 1)} \right) \tag{3.12}$$

provided $2(2N_1 + 1)^2\beta_{N_1}^{c_1-c_2} < 1/8$ and provided N_1 and $\beta_{N_1}^{c_1-c_2}$ are small enough so that above interval is a subset of $(0,1)$.

Proof. The condition (a) of Proposition 3.1 holds due to Proposition 2.4 because our assumptions guarantee that $2(2N_1 + 1)\beta_{N_1}^{c_1-c_2} < 1$.

For (b) we have to show that there exists a dual certificate $W \in \mathrm{HS}(L^2(S^1))$ satisfying (3.5). To this end we follow a similar strategy as was used in the proof of [8, Thm. 2]. Since $\mathcal{V} \cap \mathcal{W} = \{0\}$, we can choose $W = \lambda\Sigma + E_1 + E_2 \in \mathcal{V} \oplus \mathcal{W}$ with $E_1 \in \mathcal{V}$ and $E_2 \in \mathcal{W}$ such that

$$\mathcal{P}_{\mathcal{W}}W = 0 \qquad \text{and} \qquad \|\mathcal{P}_{\mathcal{V}}(\Lambda - \lambda\Sigma + W)\|_{\mathrm{HS}} \le \tfrac{\lambda}{4}\,.$$

From (3.4) we immediately obtain that

$$\|\mathcal{T}_{c_1}\Sigma\|_{\ell^\infty \times \ell^\infty} = \|\Lambda\| = 1\,, \tag{3.13}$$

and since $\mathcal{P}_{\mathcal{W}}W = 0$, we conclude that $E_2 = -\mathcal{P}_{\mathcal{W}}(\lambda\Sigma + E_1)$.

Next, we denote by $P_U : L^2(S^1) \to L^2(S^1)$ the orthogonal projection onto

$$U := \mathrm{span}\{T_{-c_2}e_n \mid |n| \le N_2\}\,.$$

Then, we can rewrite $\mathcal{P}_{\mathcal{W}}G = P_U G + G P_U - P_U G P_U$ for any $G \in \mathrm{HS}(L^2(S^1))$, which implies $\|\mathcal{P}_{\mathcal{W}}G\| \le \|P_U G\| + \|(I - P_U)G P_U\| \le 2\|G\|$. Combining this with the definition of μ and (3.13) we obtain that

$$\|E_2\| \le 2\mu(\lambda + \|\mathcal{T}_{c_1}E_1\|_{\ell^\infty \times \ell^\infty})\,. \tag{3.14}$$

Furthermore, we deduce from

$$\begin{aligned}
\frac{\lambda}{4} &\ge \|\mathcal{P}_{\mathcal{V}}(\Lambda - \lambda\Sigma + W)\|_{\mathrm{HS}} \ge -(2N_1 + 1)\|\mathcal{T}_{c_1}\mathcal{P}_{\mathcal{V}}(\Lambda + E_2)\|_{\ell^\infty \times \ell^\infty} + \|\mathcal{T}_{c_1}E_1\|_{\ell^\infty \times \ell^\infty} \\
&\ge -(2N_1 + 1)\|\mathcal{T}_{c_1}(\Lambda + E_2)\|_{\ell^\infty \times \ell^\infty} + \|\mathcal{T}_{c_1}E_1\|_{\ell^\infty \times \ell^\infty}\,,
\end{aligned}$$

the definition of ξ and (3.13) that

$$\|\mathcal{T}_{c_1}E_1\|_{\ell^\infty \times \ell^\infty} \le \frac{\lambda}{4} + (2N_1 + 1)(1 + \|E_2\|)\xi\,. \tag{3.15}$$

Combining Lemma 3.2 with the assumptions of the proposition, we obtain that

$$2(2N_1 + 1)\mu\xi < 4(2N_1 + 1)^2\beta_{N_1}^{c_1-c_2} < 1\,.$$

Accordingly, substituting (3.14) into (3.15) and solving for $\|\mathcal{T}_{c_1}E_1\|_{\ell^\infty \times \ell^\infty}$ gives

$$\|\mathcal{T}_{c_1}E_1\|_{\ell^\infty \times \ell^\infty} \le \frac{(2N_1 + 1)\xi + (2(2N_1 + 1)\mu\xi + \frac{1}{4})\lambda}{1 - 2(2N_1 + 1)\mu\xi}\,. \tag{3.16}$$

Similarly, inserting (3.16) into (3.14) yields

$$\|E_2\| \le \frac{\frac{5}{2}\mu\lambda + 2(2N_1 + 1)\mu\xi}{1 - 2(2N_1 + 1)\mu\xi}\,. \tag{3.17}$$

The definition of μ and (3.13) show that

$$\|W\| \le \mu\lambda\|\mathcal{T}_{\boldsymbol{c}_1}\Sigma\|_{\ell^\infty \times \ell^\infty} + \mu\|\mathcal{T}_{\boldsymbol{c}_1}E_1\|_{\ell^\infty \times \ell^\infty} + \|E_2\| \le \mu(\lambda + \|\mathcal{T}_{\boldsymbol{c}_1}E_1\|_{\ell^\infty \times \ell^\infty}) + \|E_2\|, \quad (3.18)$$

and using the definition of ξ and again (3.13) gives

$$\|\mathcal{T}_{\boldsymbol{c}_1}\mathcal{P}_{\mathcal{V}^\perp}(\Lambda + W)\|_{\ell^\infty \times \ell^\infty} \le \|\mathcal{T}_{\boldsymbol{c}_1}(\Lambda + E_2)\|_{\ell^\infty \times \ell^\infty} \le \xi(1 + \|E_2\|). \quad (3.19)$$

Inserting the upper bounds (3.16) and (3.17) into (3.18) and (3.19), we conclude that

$$\|W\| < \tfrac{1}{2} \qquad \text{and} \qquad \|\mathcal{T}_{\boldsymbol{c}_1}\mathcal{P}_{\mathcal{V}^\perp}(\Lambda + W)\|_{\ell^\infty \times \ell^\infty} < \tfrac{\lambda}{4}$$

if

$$\lambda \in \left(\frac{4\xi}{1 - 4(N_1 + 3)\mu\xi}, \frac{2(1 - 16(2N_1 + 1)\mu\xi)}{15\mu} \right),$$

i.e., we have constructed a dual certificate $W \in \mathrm{HS}(L^2(S^1))$ satisfying (3.5). Applying Lemma 3.2 once more finally gives (3.12). $\qquad\square$

Remark 3.4. Unfortunately, Proposition 3.3 is of limited practical relevance, as already for rather small values of $N_1 \gtrsim kR_1$, the value of $k|\boldsymbol{c}_1 - \boldsymbol{c}_2|$ must be very large for the assumptions of Proposition 3.3 to be fulfilled. However, our numerical reconstructions below illustrate that even when the assumptions of Proposition 3.3 are not fully met, far field operator splitting by principal component pursuit still gives satisfactory results. $\qquad\diamond$

Now we turn to the relaxed minimization problem (3.1) and show a stability estimate for far field operator splitting with noisy data. A related stability estimate for sparse plus low-rank matrix splitting has been established in [44, Prop. 4], and we adapt and generalize this result for the far field operator splitting problem considered here. In Theorem 3.5 below $F_q^0 \in \mathcal{V}_N^{\boldsymbol{c}_1}$ represents a discrete version of the far field operator $F_q \in \mathrm{HS}(L^2(S^1))$. Since we assume throughout this work that the whole ensemble of scatterers is compactly supported, there exists a smallest radius $R > 0$ such that $D \subseteq B_R(\boldsymbol{c}_1)$ is contained inside the ball of radius R around $\boldsymbol{c}_1$. Accordingly, the results from [22] say that choosing $N \gtrsim kR$ is sufficient to obtain an accurate best approximation of F_q in $\mathcal{V}_N^{\boldsymbol{c}_1}$. Furthermore, $F_q^\delta \in \mathcal{V}_N^{\boldsymbol{c}_1}$ denotes a discretized noisy observation of F_q. The bound δ_0 in (3.20) accounts for the approximation error of the discretization of F_q by F_q^0 and also for the modeling error $F_q - F_1 - L$ of our sparse plus low-rank ansatz from (2.9). On the other hand, the data error $F_q^0 - F_q^\delta$ is bounded by (3.21), which also guarantees (F_1, L) to be feasible for problem (3.22). We note that the only *a priori* information required by (3.22) is the approximate position $\boldsymbol{c}_1$ of the component D_1 of the scatterer.

Theorem 3.5. *Suppose that $F_q^0, F_q^\delta \in \mathcal{V}_N^{\boldsymbol{c}_1}$ for some $N \in \mathbb{N}$, and let $\boldsymbol{c}_1, \boldsymbol{c}_2 \in \mathbb{R}^2$ and $N_1, N_2 \in \mathbb{N}$ with $N_1, N_2 \le N$. Let $C_{N_1}^{\boldsymbol{c}_1 - \boldsymbol{c}_2} := 2(2N_1 + 1)\beta_{N_1}^{\boldsymbol{c}_1 - \boldsymbol{c}_2} < 1/2$ and assume that there exists a dual certificate satisfying the conditions in Proposition 3.1. Furthermore, we assume that $F_1 \in \mathcal{V}$ and $L \in \mathcal{W}$ are such that*

$$\max\big\{\|F_q^0 - (F_1 + L)\|_{\ell^1 \times \ell^1}, \|F_q^0 - (F_1 + L)\|_{\mathrm{nuc}}, \|(\mathcal{I} - \mathcal{P}_{\mathcal{V}_N^{\boldsymbol{c}_1}})L\|_{\mathrm{nuc}}\big\} \le \delta_0 \quad (3.20)$$

for some $\delta_0 \ge 0$. Suppose that $\delta > 0$ satisfies

$$\delta \ge 2\delta_0 + \|F_q^0 - F_q^\delta\|_{\mathrm{HS}} \quad (3.21)$$

and let $(F_1^\delta, L^\delta) \in \mathcal{V}_N^{\boldsymbol{c}_1} \times \mathcal{V}_N^{\boldsymbol{c}_1}$ denote the solution to

$$\underset{\widetilde{F}_1, \widetilde{L} \in \mathcal{V}_N^{\boldsymbol{c}_1}}{\text{minimize}}\ \Psi_\lambda(\widetilde{F}_1, \widetilde{L}) \qquad \text{subject to} \qquad \|F_q^\delta - (\widetilde{F}_1 + \widetilde{L})\|_{\mathrm{HS}} \le \delta. \quad (3.22)$$

13

Here, we choose $\lambda = \eta/\sqrt{2N+1} \le 1/2$ *for some* $\eta \ge 1$*. Then, there exists a constant* $C > 0$ *such that*

$$\|F_1 - F_1^\delta\|_{\mathrm{HS}}^2 \le C\Big(1 + \big(1 + (1 - C_{N_1}^{\boldsymbol{c}_1 - \boldsymbol{c}_2})^{-1}\big)(2N+1)^2\Big)\delta^2 \tag{3.23a}$$

and

$$\|L - L^\delta\|_{\mathrm{HS}}^2 \le C\Big(1 + \big(1 + (1 - C_{N_1}^{\boldsymbol{c}_1 - \boldsymbol{c}_2})^{-1}\big)(2N+1)^2\Big)\delta^2 . \tag{3.23b}$$

Proof. We use the notations $\widehat{F}_1 := F_1 - F_1^\delta$, $\widehat{L} := L - L^\delta$, $\widehat{G}^+ := (\widehat{F}_1 + \widehat{L})/2$ and $\widehat{G}^- := (\widehat{F}_1 - \widehat{L})/2$. From the parallelogram identity we conclude

$$\begin{aligned}
\|\widehat{F}_1\|_{\mathrm{HS}}^2 , \|\widehat{L}\|_{\mathrm{HS}}^2 &\le \|\widehat{F}_1\|_{\mathrm{HS}}^2 + \|\widehat{L}\|_{\mathrm{HS}}^2 = 2\|\widehat{G}^+\|_{\mathrm{HS}}^2 + 2\|\widehat{G}^-\|_{\mathrm{HS}}^2 \\
&= 2\|\widehat{G}^+\|_{\mathrm{HS}}^2 + \big(\|\mathcal{P}_\mathcal{V}\widehat{G}^-\|_{\mathrm{HS}}^2 + \|\mathcal{P}_\mathcal{W}\widehat{G}^-\|_{\mathrm{HS}}^2\big) + \big(\|\mathcal{P}_{\mathcal{V}^\perp}\widehat{G}^-\|_{\mathrm{HS}}^2 + \|\mathcal{P}_{\mathcal{W}^\perp}\widehat{G}^-\|_{\mathrm{HS}}^2\big) .
\end{aligned} \tag{3.24}$$

In the following, we bound the three terms on the right hand side of (3.24) separately.

Applying (3.20), (3.21) and the fact that $\|\cdot\|_{\mathrm{HS}} \le \|\cdot\|_{\mathrm{nuc}}$ we obtain for the first term on the right hand side of (3.24) that

$$\begin{aligned}
2\|\widehat{G}^+\|_{\mathrm{HS}}^2 &\le \tfrac{1}{2}\big(\|F_q^0 - (F_1 + L)\|_{\mathrm{HS}} + \|F_q^0 - F_q^\delta\|_{\mathrm{HS}} + \|F_q^\delta - (F_1^\delta + L^\delta)\|_{\mathrm{HS}}\big)^2 \\
&\le \tfrac{1}{2}(2\delta - \delta_0)^2 \le 2\delta^2 .
\end{aligned} \tag{3.25}$$

To bound the second term on the right hand side of (3.24) we note first that, using (2.16),

$$\begin{aligned}
\|\mathcal{P}_\mathcal{V}\widehat{G}^- - \mathcal{P}_\mathcal{W}\widehat{G}^-\|_{\mathrm{HS}}^2 &\ge \|\mathcal{P}_\mathcal{V}\widehat{G}^-\|_{\mathrm{HS}}^2 + \|\mathcal{P}_\mathcal{W}\widehat{G}^-\|_{\mathrm{HS}}^2 - 2|\langle\mathcal{P}_\mathcal{V}\widehat{G}^-, \mathcal{P}_\mathcal{W}\widehat{G}^-\rangle|_{\mathrm{HS}} \\
&\ge \|\mathcal{P}_\mathcal{V}\widehat{G}^-\|_{\mathrm{HS}}^2 + \|\mathcal{P}_\mathcal{W}\widehat{G}^-\|_{\mathrm{HS}}^2 - 2C_{N_1}^{\boldsymbol{c}_1 - \boldsymbol{c}_2}\|\mathcal{P}_\mathcal{V}\widehat{G}^-\|_{\mathrm{HS}}\|\mathcal{P}_\mathcal{W}\widehat{G}^-\|_{\mathrm{HS}} \\
&\ge (1 - C_{N_1}^{\boldsymbol{c}_1 - \boldsymbol{c}_2})\big(\|\mathcal{P}_\mathcal{V}\widehat{G}^-\|_{\mathrm{HS}}^2 + \|\mathcal{P}_\mathcal{W}\widehat{G}^-\|_{\mathrm{HS}}^2\big) .
\end{aligned}$$

Dividing this inequality by $1 - C_{N_1}^{\boldsymbol{c}_1 - \boldsymbol{c}_2}$, which is valid since we assumed that $C_{N_1}^{\boldsymbol{c}_1 - \boldsymbol{c}_2} < 1/2$, and estimating further gives

$$\begin{aligned}
\|\mathcal{P}_\mathcal{V}\widehat{G}^-\|_{\mathrm{HS}}^2 + \|\mathcal{P}_\mathcal{W}\widehat{G}^-\|_{\mathrm{HS}}^2 &\le \tfrac{1}{1 - C_{N_1}^{\boldsymbol{c}_1 - \boldsymbol{c}_2}}\|\mathcal{P}_\mathcal{V}\widehat{G}^- - \mathcal{P}_\mathcal{W}\widehat{G}^-\|_{\mathrm{HS}}^2 \\
&= \tfrac{1}{1 - C_{N_1}^{\boldsymbol{c}_1 - \boldsymbol{c}_2}}\|\mathcal{P}_{\mathcal{V}^\perp}\widehat{G}^- - \mathcal{P}_{\mathcal{W}^\perp}\widehat{G}^-\|_{\mathrm{HS}}^2 \le \tfrac{2}{1 - C_{N_1}^{\boldsymbol{c}_1 - \boldsymbol{c}_2}}\big(\|\mathcal{P}_{\mathcal{V}^\perp}\widehat{G}^-\|_{\mathrm{HS}}^2 + \|\mathcal{P}_{\mathcal{W}^\perp}\widehat{G}^-\|_{\mathrm{HS}}^2\big) ,
\end{aligned} \tag{3.26}$$

i.e., it remains to establish a bound for the third term on the right hand side of (3.24).

Using the isometry property of $\boldsymbol{\mathcal{T}}_{\boldsymbol{c}_1}$ on $\mathrm{HS}(L^2(S^1))$ and the estimates $\|\cdot\|_{\mathrm{HS}} \le \|\cdot\|_{\mathrm{nuc}}$ and $\|\cdot\|_{\mathrm{HS}} \le \|\cdot\|_{\ell^1 \times \ell^1}$ it follows for $\lambda \ge 1/\sqrt{2N+1}$ that

$$\begin{aligned}
\|\mathcal{P}_{\mathcal{V}^\perp}\widehat{G}^-\|_{\mathrm{HS}}^2 + \|\mathcal{P}_{\mathcal{W}^\perp}\widehat{G}^-\|_{\mathrm{HS}}^2 &\le \big(\|\mathcal{P}_{\mathcal{V}^\perp}\widehat{G}^-\|_{\mathrm{HS}} + \|\mathcal{P}_{\mathcal{W}^\perp}\widehat{G}^-\|_{\mathrm{HS}}\big)^2 \\
&\le (2N+1)\big(\Psi_\lambda(\mathcal{P}_{\mathcal{V}^\perp}\widehat{G}^-, \mathcal{P}_{\mathcal{W}^\perp}\widehat{G}^-)\big)^2 .
\end{aligned} \tag{3.27}$$

Since $(F_1, \mathcal{P}_{\mathcal{V}_N^{\boldsymbol{c}_1}}L)$ is feasible for (3.22) by (3.20), we conclude using (3.20) once more that

$$\Psi_\lambda(F_1 - \widehat{F}_1, L - \widehat{L}) = \Psi_\lambda(F_1^\delta, L^\delta) \le \Psi_\lambda(F_1, \mathcal{P}_{\mathcal{V}_N^{\boldsymbol{c}_1}}L) \le \Psi_\lambda(F_1, L) + \delta_0 . \tag{3.28}$$

Next we use (3.11) with $G = \widehat{G}^-$, which is valid since we assumed the assumptions of Proposition 3.1 to be satisfied, and recall that $\lambda \le 1/2$ to conclude that

$$\begin{aligned}
\Psi_\lambda(F_1 - \widehat{G}^-, L + \widehat{G}^-) - \psi_\lambda(F_1, L) &\ge \tfrac{1}{2}\Big(\lambda\|\boldsymbol{\mathcal{T}}_{\boldsymbol{c}_1}\mathcal{P}_{\mathcal{V}^\perp}\widehat{G}^-\|_{\ell^1 \times \ell^1} + \tfrac{1}{2}\|\mathcal{P}_{\mathcal{W}^\perp}\widehat{G}^-\|_{\mathrm{nuc}}\Big) \\
&\ge \tfrac{1}{4}\Psi_\lambda(\mathcal{P}_{\mathcal{V}^\perp}\widehat{G}^-, \mathcal{P}_{\mathcal{W}^\perp}\widehat{G}^-) .
\end{aligned}$$

Consequently, we obtain by rewriting $\widehat{G}^- = \widehat{F}_1 - \widehat{G}^+ = -\widehat{L} + \widehat{G}^+$ that

$$
\begin{aligned}
\Psi_\lambda(\mathcal{P}_{\mathcal{V}^\perp}\widehat{G}^-, \mathcal{P}_{\mathcal{W}^\perp}\widehat{G}^-) &\leq 4\big(\Psi_\lambda(F_1 - \widehat{G}^-, L + \widehat{G}^-) - \psi_\lambda(F_1, L)\big) \\
&\leq 4\big(\Psi_\lambda(F_1 - \widehat{F}_1, L - \widehat{L}) - \big(\Psi_\lambda(F_1, L) + \delta_0\big) + \big(\Psi_\lambda(\widehat{G}^+, \widehat{G}^+) + \delta_0\big)\big) \quad (3.29) \\
&\leq 4\big(\Psi_\lambda(\widehat{G}^+, \widehat{G}^+) + \delta_0\big),
\end{aligned}
$$

where we have used (3.28) in the last step. Now we insert (3.29) into (3.27) to deduce

$$
\begin{aligned}
\|\mathcal{P}_{\mathcal{V}^\perp}\widehat{G}^-\|_{\mathrm{HS}}^2 + \|\mathcal{P}_{\mathcal{W}^\perp}\widehat{G}^-\|_{\mathrm{HS}}^2 &\leq 16(2N+1)\big(\Psi_\lambda(\widehat{G}^+, \widehat{G}^+) + \delta_0\big)^2 \\
&\leq 4(2N+1)\big(\Psi_\lambda(F_q^0 - (F_1^\delta + L^\delta), F_q^0 - (F_1^\delta + L^\delta)) \quad (3.30) \\
&\qquad + \Psi_\lambda(F_q^0 - (F_1 + L), F_q^0 - (F_1 + L)) + 2\delta_0\big)^2.
\end{aligned}
$$

Since $\|\cdot\|_{\mathrm{nuc}} \leq \sqrt{2N+1}\|\cdot\|_{\mathrm{HS}}$ and $\|\mathcal{T}_{\boldsymbol{c}_1}(\cdot)\|_{\ell^1 \times \ell^1} \leq (2N+1)\|\cdot\|_{\mathrm{HS}}$ on $\mathcal{V}_N^{\boldsymbol{c}_1}$, we can use (3.20) and (3.21) to obtain

$$
\Psi_\lambda(F_q^0 - (F_1^\delta + L^\delta), F_q^0 - (F_1^\delta + L^\delta)) \leq 2\big(\sqrt{2N+1} + \lambda(2N+1)\big)(\delta - \delta_0).
$$

Similarly,

$$
\Psi_\lambda(F_q^0 - (F_1 + L), F_q^0 - (F_1 + L)) \leq (1 + \lambda)\delta_0.
$$

Substituting the last two inequalities into (3.30) gives

$$
\begin{aligned}
&\|\mathcal{P}_{\mathcal{V}^\perp}\widehat{G}^-\|_{\mathrm{HS}}^2 + \|\mathcal{P}_{\mathcal{W}^\perp}\widehat{G}^-\|_{\mathrm{HS}}^2 \\
&\leq 4(2N+1)\big(2(\sqrt{2N+1} + \lambda(2N+1))\delta - (2\sqrt{2N+1} + \lambda(4N+1) - 3)\delta_0\big)^2 \quad (3.31) \\
&\leq 16(2N+1)\big(\sqrt{2N+1} + \lambda(2N+1)\big)^2 \delta^2.
\end{aligned}
$$

Finally, we insert (3.25), (3.26) and (3.31) into (3.24) to obtain

$$
\|F_1 - F_1^\delta\|_{\mathrm{HS}}^2, \; \|L - L^\delta\|_{\mathrm{HS}}^2 \leq \big(2 + (1 + 2(1 - C_{N_1}^{\boldsymbol{c}_1 - \boldsymbol{c}_2})^{-1})16(2N+1)(\sqrt{2N+1} + \lambda(2N+1))^2\big)\delta^2,
$$

which implies (3.23) by our choice of λ. $\qquad\square$

4 Numerical examples

Now we briefly comment on the numerical implementation of far field operator splitting by principal component pursuit as discussed in the previous section. Following [43] we consider a slightly relaxed version of (3.1), in which the inequality constraint is replaced by a penalty term. Accordingly, we aim to solve

$$
\underset{\widetilde{F}_1, \widetilde{L} \in \mathcal{V}_N^{\boldsymbol{c}_1}}{\text{minimize}} \|F_q^\delta - (\widetilde{F}_1 + \widetilde{L})\|_{\mathrm{HS}}^2 + \mu\big(\lambda\|\mathcal{T}_{\boldsymbol{c}_1}\widetilde{F}_1\|_{\ell^1 \times \ell^1} + \|\widetilde{L}\|_{\mathrm{nuc}}\big), \quad (4.1)
$$

where $\mu > 0$ is a small constant. We use a proximal gradient approach as proposed in [35, 43] to approximate the unique solution of (4.1).

In all our numerical examples the contrast function is chosen to be $q = \chi_{D_1} - 0.5\chi_{D_2}$ with two scatterers $D_1 \subset B_{R_1}(\boldsymbol{c}_1)$ and $D_2 \subset B_{R_2}(\boldsymbol{c}_2)$ as shown in Figure 2.1 (left), and we use $k = 1$ for the wave number. We simulate the associated far field operators F_q and F_{q_1} using a Nyström method with $M = 170$ equidistant illumination and observation directions on S^1 as described in Example 2.1. Here, the number of sampling points M has been chosen such that all far field operators in the examples below can be fully resolved.
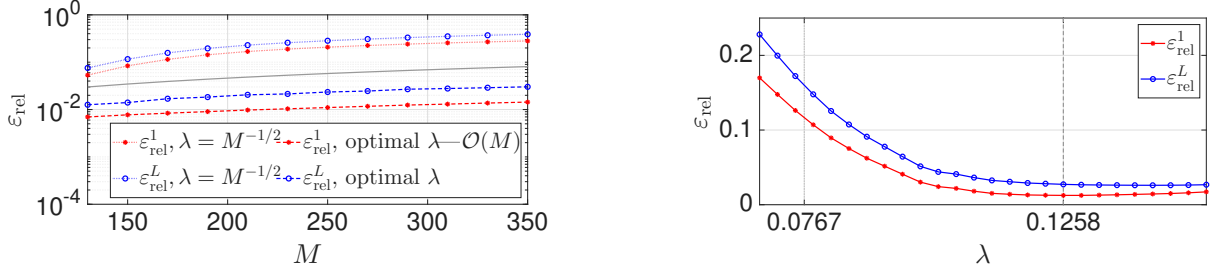
Figure 4.1: Left: Relative reconstruction errors for varying number M of discretization points for $\lambda = M^{-1/2}$ and for optimally chosen λ in Example 4.1. Right: Relative reconstruction errors for fixed $M = 170$ and varying λ. Typically proposed choice $\lambda = M^{-1/2} \approx 0.077$ from literature and optimal choice $\lambda \approx 0.13$ marked by vertical grey lines.

Denoting in the following the numerical solutions of (4.1) by $(\widehat{F}_1, \widehat{L})$, we will evaluate the relative reconstruction errors

$$\varepsilon_{\mathrm{rel}}^1 := \frac{\|F_{q_1} - \widehat{F}_1\|_{\mathrm{HS}}}{\|F_{q_1}\|_{\mathrm{HS}}} \qquad \text{and} \qquad \varepsilon_{\mathrm{rel}}^L := \frac{\|(F_q - F_{q_1}) - \widehat{L}\|_{\mathrm{HS}}}{\|F_q - F_{q_1}\|_{\mathrm{HS}}}$$

to assess the quality of these numerical solutions. The *a priori* information $\boldsymbol{c}_1 = (-28, -30)^\top$ on the approximate location of the scatterer D_1 that enters the reconstruction algorithm is marked by a cross inside D_1 in Figure 2.1 (left).

We note that the assumptions of Theorem 3.5 are not satisfied for the particular setup discussed in this section. However, we will see that the splitting algorithm still gives good reconstructions.

Example 4.1 (Choice of coupling parameter λ)**.** In our first example, we study the optimal choice of the coupling parameter λ in (4.1) depending on the number of incident and observation directions M used to approximate the far field operators. To this end we vary M between $M = 130$ and $M = 350$, always using $\mu = 3 \times 10^{-4} M/\lambda$ for the second parameter in (4.1).

In the literature often the value $\lambda = M^{-1/2}$ is used (see, e.g., [7, 44]). This is also the smallest possible choice of λ that is covered by our stability Theorem 3.5. However, since a larger choice of λ promotes a better reconstruction quality for the sparse component F_1, it makes sense to choose λ slightly larger. We have determined the corresponding optimal values for λ depending on M by minimizing the associated relative reconstruction error $\varepsilon_{\mathrm{rel}}^1$ of the sparse component. The results are shown in Figure 4.1 (left). It turns out that choosing $\lambda \approx 2M^{-1/2}$ always produces better reconstructions. For all error curves in Figure 4.1 (left) we observe an increase of the order $\mathcal{O}(M)$ with respect to M, as to be expected from (3.23).

Figure 4.1 (right) shows the relative reconstruction errors depending on the coupling parameter λ for fixed number of incident and observation directions $M = 170$. The literature value $\lambda = M^{-1/2} \approx 0.0767$ as well as our optimized choice $\lambda \approx 0.1258$ are marked by vertical gray lines. $\diamondsuit$

Example 4.2 (Varying noise level δ)**.** We consider the same setting as in the previous example with fixed $M = 170$ and choose accordingly $\lambda = 0.13$. In this example we study the quality of our reconstructions when complex valued uniformly distributed relative error is being added to the simulated far field operators F_q. Denoting by $\delta_{\mathrm{rel}} \in (0, 0.1)$ the relative noise level, we generate 15 different random noise realizations for each noise level and plot the relative reconstruction errors of the worst reconstructions in Figure 4.2. We note that larger noise levels require more regularization, and accordingly the parameter μ in (4.1) has been increased
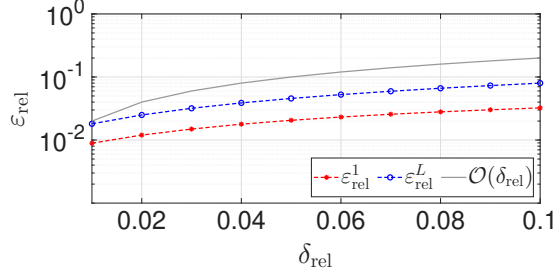
16

Figure 4.2: Worst relative reconstruction errors for varying relative noise level δ_{rel} after 15 runs in Example 4.2.
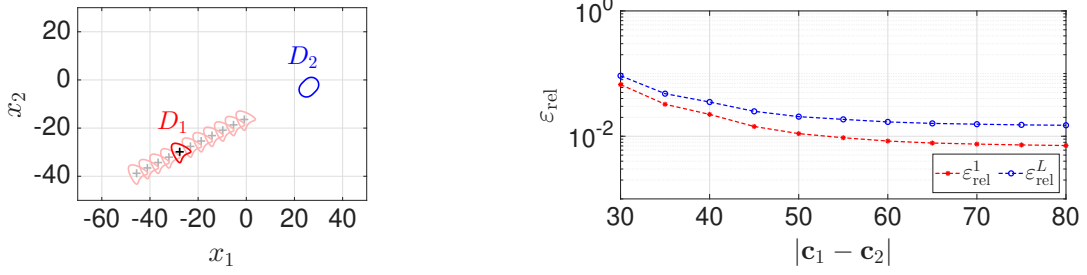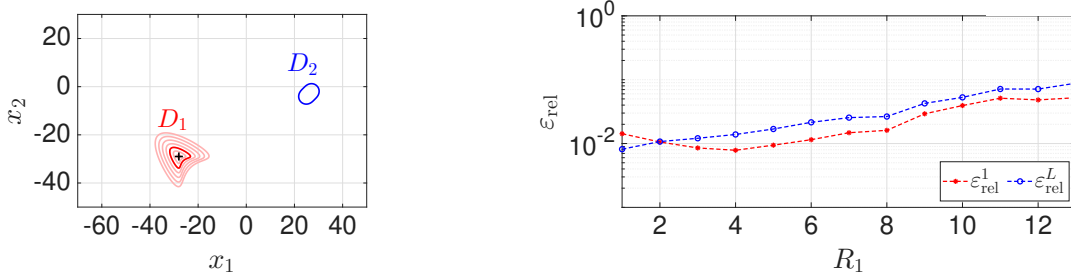

Figure 4.3: Left: Geometry of two scatterers (red, blue) and *a priori* information on location c_1 of first scatterer (black +) for varying distance $|c_1 - c_2|$ in Example 4.3. Right: Relative reconstruction errors for varying distance $|c_1 - c_2|$ in Example 4.3.

from $\mu = 3 \times 10^{-4} M/\lambda$ for $\delta_{\mathrm{rel}} = 0$ to $\mu = 1.2 \times 10^{-3} M/\lambda$ for $\delta_{\mathrm{rel}} = 0.1$ in these calculations. As soon as the additive random noise dominates the modeling error, both error curves in Figure 4.2 increase with a rate of order $\mathcal{O}(\delta_{\mathrm{rel}})$ with respect to δ_{rel}, as expected from (3.23). $\diamondsuit$

Example 4.3 (Varying distance between and diameter of scatterers)**.** In our third example, we study the dependence of the performance of our method depending on the distance $|c_1 - c_2|$ between the two components of the scatterer and on the size parameters R_1 and R_2. In our stability estimates (3.23) these dependencies are hidden in the constant $C_{N_1}^{c_1 - c_2}$ (see also the last estimate at the end of the proof of Theorem 3.5). Accordingly, the accuracy of the numerical reconstructions should improve with increasing distance and with decreasing radii. Our estimates also suggest that the relative reconstruction errors should grow faster for increasing R_1 than for increasing R_2. In our numerical tests below, we use $M = 170$ and choose $\mu = 3 \times 10^{-4} M/\lambda$.

We start by varying the distance $|c_1 - c_2|$ between the scatterers. To this end we keep the position c_2 of the nut-shaped scatterer D_2 fixed and vary the position c_1 of the kite-shaped scatterer D_1, as shown in Figure 4.3 (left). The resulting relative reconstruction errors with optimally chosen coupling parameter λ (see Example 4.1) are shown in Figure 4.3 (right). As expected, both relative errors decrease with increasing distance $|c_1 - c_2|$.

In order to analyze the quality of our reconstructions depending on the size of the scatterers, we fix one of the two and vary the size of the other. In both tests, we select the coupling parameter λ optimally (see Example 4.1). We start by varying the size R_1 of the kite-shaped scatterer as shown in Figure 4.4 (left), where its instance for $R_1 = 5$ is highlighted. The associated relative reconstruction errors are plotted in Figure 4.4 (right). For $R_1 \geq 4$ both error curves increase with increasing R_1, as expected. For $R_1 < 4$, the relative error $\varepsilon_{\mathrm{rel}}^1$ increases as R_1 decreases. At $R_1 = 1$, the low-rank component L is reconstructed even better than the sparse component F_1. This behavior is probably due to the fact that for R_1 very small q_2 scatters much stronger than q_1. Finally, we vary the size R_2 of the nut-shaped scatterer as shown in

17

Figure 4.4: Left: Geometry of two scatterers (red, blue) and *a priori* information on location c_1 of first scatterer (black +) for varying size R_1 of kite-shaped scatterer in Example 4.3. Right: Relative reconstruction errors for varying size R_1 in Example 4.3.
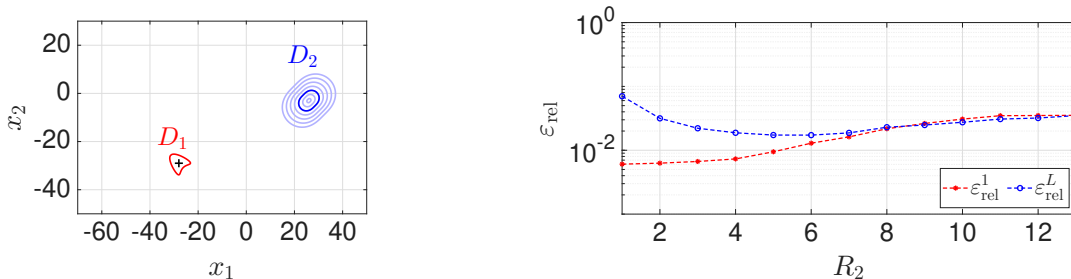

Figure 4.5: Left: Geometry of two scatterers (red, blue) and *a priori* information on location c_1 of first scatterer (black +) for varying size R_2 of nut-shaped scatterer in Example 4.3. Right: Relative reconstruction errors for varying size R_2 in Example 4.3.

Figure 4.5 (left). Again the instance corresponding to $R_2 = 5$ is highlighted. The associated relative reconstruction errors can be found in Figure 4.4 (right). As expected, we observe $\varepsilon_{\mathrm{rel}}^1$ to grow with R_2. It can also be seen, that increasing R_1 has a stronger effect on the relative reconstruction error than increasing R_2. $\diamondsuit$

Conclusions

We have developed a new method to separate or split off the scattering data associated to a single scatterer that is part of an ensemble of well-separated scatterers from the scattering data for the whole ensemble. This question arises for instance when one wishes to recover properties of scatterers in a certain focus area while not being interested in scatterers outside this region so much. Using sparsity and low-rank properties of far field operators associated to compactly supported scatterers, we have shown that a convex program called principle component pursuit can be utilized to approximate solutions to this inverse problem. Our main theoretical result is a stability estimate for this method taking into account modeling errors and data noise. We have put particular emphasis on expressing the prerequisites of this theorem and the associated stability constants solely in terms of geometric properties of the scattering ensemble and the wave length. Although the assumptions of our theoretical results are quite restrictive, the numerical results confirm that the reconstruction algorithm also works well if these assumptions are not fully met.

Acknowledgments

References

[1] L. Audibert and H. Haddar. A generalized formulation of the linear sampling method with exact characterization of targets in terms of farfield measurements. *Inverse Problems*, 30(3):035011, 20, 2014. `doi:10.1088/0266-5611/30/3/035011`.

[2] D. Baffet and M. J. Grote. On wave splitting, source separation and echo removal with absorbing boundary conditions. *J. Comput. Phys.*, 387:589–596, 2019. `doi:10.1016/j.jcp.2019.03.004`.

[3] F. ben Hassen, J. Liu, and R. Potthast. On source analysis by wave splitting with applications in inverse scattering of multiple obstacles. *J. Comput. Math.*, 25(3):266–281, 2007.

[4] A. L. Bukhgeim. Recovering a potential from Cauchy data in the two-dimensional case. *J. Inverse Ill-Posed Probl.*, 16(1):19–33, 2008. `doi:10.1515/jiip.2008.002`.

[5] F. Cakoni and D. Colton. *A qualitative approach to inverse scattering theory.* Springer, New York, 2014. `doi:10.1007/978-1-4614-8827-9`.

[6] F. Cakoni, D. Colton, and H. Haddar. *Inverse scattering theory and transmission eigenvalues*, volume 98 of *CBMS-NSF Regional Conference Series in Applied Mathematics*. Society for Industrial and Applied Mathematics (SIAM), Philadelphia, PA, second edition, 2023.

[7] E. J. Candès, X. Li, Y. Ma, and J. Wright. Robust principal component analysis? *J. ACM*, 58(3):Art. 11, 37, 2011. `doi:10.1145/1970392.1970395`.

[8] V. Chandrasekaran, S. Sanghavi, P. A. Parrilo, and A. S. Willsky. Rank-sparsity incoherence for matrix decomposition. *SIAM J. Optim.*, 21(2):572–596, 2011. `doi:10.1137/090761793`.

[9] S. S. Chen, D. L. Donoho, and M. A. Saunders. Atomic decomposition by basis pursuit. *SIAM J. Sci. Comput.*, 20(1):33–61, 1998. `doi:10.1137/S1064827596304010`.

[10] S. Cogar, D. Colton, S. Meng, and P. Monk. Modified transmission eigenvalues in inverse scattering theory. *Inverse Problems*, 33(12):125002, 31, 2017. `doi:10.1088/1361-6420/aa9418`.

[11] D. Colton and A. Kirsch. A simple method for solving inverse scattering problems in the resonance region. *Inverse Problems*, 12(4):383–393, 1996. `doi:10.1088/0266-5611/12/4/003`.

[12] D. Colton and R. Kress. Eigenvalues of the far field operator for the Helmholtz equation in an absorbing medium. *SIAM J. Appl. Math.*, 55(6):1724–1735, 1995. `doi:10.1137/S0036139993256114`.

[13] D. Colton and R. Kress. *Inverse acoustic and electromagnetic scattering theory.* Springer, Cham, fourth edition, 2019. `doi:10.1007/978-3-030-30351-8`.

[14] D. Colton and P. Monk. The inverse scattering problem for time-harmonic acoustic waves in an inhomogeneous medium. *Quart. J. Mech. Appl. Math.*, 41(1):97–125, 1988. `doi:10.1093/qjmam/41.1.97`.

[15] F. Deutsch. The angle between subspaces of a Hilbert space. In *Approximation theory, wavelets and applications (Maratea, 1994)*, volume 454 of *NATO Adv. Sci. Inst. Ser. C: Math. Phys. Sci.*, pages 107–130. Kluwer Acad. Publ., Dordrecht, 1995.

[16] *NIST Digital Library of Mathematical Functions.* `https://dlmf.nist.gov/`, Release 1.2.2 of 2024-09-15. F. W. J. Olver, A. B. Olde Daalhuis, D. W. Lozier, B. I. Schneider, R. F. Boisvert, C. W. Clark, B. R. Miller, B. V. Saunders, H. S. Cohl, and M. A. McClain, eds. URL: `https://dlmf.nist.gov/`.

[17] D. L. Donoho, M. Elad, and V. N. Temlyakov. Stable recovery of sparse overcomplete representations in the presence of noise. *IEEE Trans. Inform. Theory*, 52(1):6–18, 2006. `doi:10.1109/TIT.2005.860430`.

[18] D. L. Donoho and X. Huo. Uncertainty principles and ideal atomic decomposition. *IEEE Trans. Inform. Theory*, 47(7):2845–2862, 2001. `doi:10.1109/18.959265`.

[19] M. Graff, M. J. Grote, F. Nataf, and F. Assous. How to solve inverse scattering problems without knowing the source term: a three-step strategy. *Inverse Problems*, 35(10):104001, 20, 2019. `doi:10.1088/1361-6420/ab2d5f`.

[20] R. Griesmaier, M. Hanke, and J. Sylvester. Far field splitting for the Helmholtz equation. *SIAM J. Numer. Anal.*, 52(1):343–362, 2014. `doi:10.1137/120891381`.

[21] R. Griesmaier and B. Harrach. Monotonicity in inverse medium scattering on unbounded domains. *SIAM J. Appl. Math.*, 78(5):2533–2557, 2018. `doi:10.1137/18M1171679`.

[22] R. Griesmaier and L. Schätzle. Far field operator splitting and completion in inverse medium scattering. *Inverse Problems*, 40(11):Paper No. 115010, 32, 2024. `doi:10.1088/1361-6420/ad7c77`.

[23] R. Griesmaier and J. Sylvester. Far field splitting by iteratively reweighted ℓ^1 minimization. *SIAM J. Appl. Math.*, 76(2):705–730, 2016. `doi:10.1137/15M102839X`.

[24] R. Griesmaier and J. Sylvester. Uncertainty principles for inverse source problems, far field splitting, and data completion. *SIAM J. Appl. Math.*, 77(1):154–180, 2017. `doi:10.1137/16M1086157`.

[25] R. Griesmaier and J. Sylvester. Uncertainty principles for three-dimensional inverse source problems. *SIAM J. Appl. Math.*, 77(6):2066–2092, 2017. `doi:10.1137/17M111287X`.

[26] R. Griesmaier and J. Sylvester. Uncertainty principles for inverse source problems for electromagnetic and elastic waves. *Inverse Problems*, 34(6):065003, 37, 2018. `doi:10.1088/1361-6420/aab45c`.

[27] D. Gross. Recovering low-rank matrices from few coefficients in any basis. *IEEE Trans. Inform. Theory*, 57(3):1548–1566, 2011. `doi:10.1109/TIT.2011.2104999`.

[28] M. J. Grote, M. Kray, F. Nataf, and F. Assous. Time-dependent wave splitting and source separation. *J. Comput. Phys.*, 330:981–996, 2017. `doi:10.1016/j.jcp.2016.10.021`.

[29] K. Kilgore, S. Moskow, and J. C. Schotland. Inverse Born series for scalar waves. *J. Comput. Math.*, 30(6):601–614, 2012. `doi:10.4208/jcm.1205-m3935`.

[30] A. Kirsch. Characterization of the shape of a scattering obstacle using the spectral data of the far field operator. *Inverse Problems*, 14(6):1489–1512, 1998. `doi:10.1088/0266-5611/14/6/009`.

[31] A. Kirsch. Remarks on the Born approximation and the factorization method. *Appl. Anal.*, 96(1):70–84, 2017. `doi:10.1080/00036811.2016.1188286`.

[32] A. Kirsch. *An introduction to the mathematical theory of inverse problems*. Springer, third edition, 2021. `doi:10.1007/978-3-030-63343-1`.

[33] A. Kirsch and N. Grinberg. *The factorization method for inverse problems*. Oxford University Press, Oxford, 2008.

[34] I. Krasikov. Uniform bounds for Bessel functions. *J. Appl. Anal.*, 12(1):83–91, 2006. `doi:10.1515/JAA.2006.83`.

[35] Z. Lin, A. Ganesh, J. Wright, L. Wu, M. Chen, and Y. Ma. Fast convex optimization algorithms for exact recovery of a corrupted low-rank matrix. *Coordinated Science Laboratory Report no. UILU-ENG-09-2214, DC-246*, 2009.

[36] A. I. Nachman. Reconstructions from boundary measurements. *Ann. of Math. (2)*, 128(3):531–576, 1988. `doi:10.2307/1971435`.

[37] F. Natterer. An error bound for the Born approximation. *Inverse Problems*, 20(2):447–452, 2004. `doi:10.1088/0266-5611/20/2/009`.

[38] R. G. Novikov. A multidimensional inverse spectral problem for the equation $-\Delta\psi + (v(x) - Eu(x))\psi = 0$. *Funktsional. Anal. i Prilozhen.*, 22(4):11–22, 96, 1988. `doi:10.1007/BF01077418`.

[39] R. Potthast, F. M. Fazi, and P. A. Nelson. Source splitting via the point source method. *Inverse Problems*, 26(4):045002, 17, 2010. `doi:10.1088/0266-5611/26/4/045002`.

[40] A. G. Ramm. Recovery of the potential from fixed-energy scattering data. *Inverse Problems*, 4(3):877–886, 1988. URL: `http://stacks.iop.org/0266-5611/4/877`.

[41] J. Sylvester. An estimate for the free Helmholtz equation that scales. *Inverse Probl. Imaging*, 3(2):333–351, 2009. `doi:10.3934/ipi.2009.3.333`.

[42] F. Triki and M. Karamehmedović. On the series solutions of integral equations in scattering. *C. R. Math. Acad. Sci. Paris*, 362:1023–1035, 2024. `doi:10.5802/crmath.621`.

[43] J. Wright, A. Ganesh, S. Rao, Y. Peng, and Y. Ma. Robust principal component analysis: Exact recovery of corrupted low-rank matrices via convex optimization. In Y. Bengio, D. Schuurmans, J. Lafferty, C. Williams, and A. Culotta, editors, *Advances in Neural Information Processing Systems*, volume 22. Curran Associates, Inc., 2009.

[44] Z. Zhou, X. Li, J. Wright, E. Candès, and Y. Ma. Stable principal component pursuit. In *2010 IEEE International Symposium on Information Theory*, pages 1518–1522, 2010. `doi:10.1109/ISIT.2010.5513535`.